was dispensable for the anti-HBV effect, as PSC833, a CsA derivative inactive for CN inhibition (Fig. 4B),[18] could still inhibit HBV infection (Fig. 4C). As PSC833 and FK506 did not bind to the active site of CyPs (Fig. 4D), CyP inhibition is not likely to be responsible for the anti-HBV activity.

CsA Blocked HBV Infection Through Targeting NTCP. Recently, NTCP was reported as a candidate entry receptor for HBV.[22] A transporter activity assay showed that CsA inhibited the activity of NTCP both in 293 (Fig. 5A) and HepG2 cells (Fig. 5B) engineered to stably overexpress NTCP, as previously reported.[35] CsA was also suggested to bind to NTCP on the membrane in a ligand binding assay using HepG2-NTCP cells (Fig. S2).

NTCP messenger RNA (mRNA) was expressed in HepaRG cells and PHH, which are HBV-susceptible, while little to no expression was detected in HBV-nonsusceptible cell lines including HepG2, Huh-7, FLC4, and nonhepatocyte HeLa cells (Fig. 5C). In contrast, CyPA and CyPB were expressed in all of these cell lines, irrespective of infection susceptibility. Intriguingly, we found that the inhibition of NTCP transporter activity correlated with anti-HBV entry activity (Figs. 5A, 4A,B). These results suggest the possibility that compounds targeting NTCP have the potential to block HBV infection. To test this prediction, we treated HepaRG cells with compounds known to inhibit NTCP, including ursodeoxycholate, cholic acid, propranolol, progesterone, and bosentan[35,36] to investigate the effect on HBV entry using the protocol in Fig. 1A. As shown in Fig. 5D, these compounds inhibited HBV infection. Thus, inhibition of NTCP blocked HBV infection. We also showed that HepG2 cells overexpressing NTCP were susceptible to HBV infection (Fig. 5E), as reported recently.[22] Treatment with CsA also reduced HBs and HBe secretion when these cells were infected with HBV (Fig. 5E), suggesting that CsA inhibited NTCP-mediated HBV infection.

The binding of the HBV large envelope protein (LHBs) to NTCP was reported to be important for HBV entry.[22] Thus, one mechanism by which compounds that directly inhibit NTCP activity may block HBV entry is interruption of the binding between NTCP and LHBs. To test this possibility, we established an AlphaScreen assay to evaluate LHBs-NTCP binding *in vitro* as described in the Materials and Methods. *In vitro* synthesized NTCP and LHBs were at least partially functional, as NTCP bound to its substrate TCA (Fig. S3A) and LHBs could neutralize HBV infection into HepaRG cells (Fig. S3B). As shown in Fig. 5F, incubation of recombinant NTCP with LHBs but not middle (MHBs) and small envelope protein (SHBs) produced a significant AlphaScreen signal (Fig. 5F-a, left) indicative of a direct protein-protein interaction. In contrast to NTCP, recombinant GST or other nonrelevant proteins, LCK and FYN,[37] did not produce a binding signal when incubated with LHBs (Fig. 5F-a), suggesting that our AlphaScreen assay produced a specific signal for the interaction of NTCP with LHBs. Consistent with the report that the pre-S1 region of LHBs was important for the binding to NTCP,[22] the signal was decreased in a dose-dependent manner by the addition of pre-S1 lipopeptide HBVpreS/2-48^{myr,5} (Fig. 5F-b) but not of an inactive mutant of pre-S1 (Fig. S3C), indicating a competition of pre-S1 with LHBs for NTCP binding. In this assay, CsA as well as FK506 and a CsA derivative, SCYX1454139 (see the next section), were shown to reduce the signal for LHBs-NTCP binding in a dose-dependent manner (Fig. 5F-c,d,e). These results suggest that CsA targets NTCP and thereby inhibits the interaction between LHBs and NTCP.

Identification of CsA Analogs Possessing a Higher Anti-HBV Potential. Considering CsA as a lead compound, we tested CsA analogs for anti-HBV activity. As shown in Fig. 6A, SCYX618806 reduced HBs secretion after HBV infection, while a related analog SCYX1774198 did not have a significant anti-HBV effect (Fig. 6A,C). Additional analogs, SCYX827830 and SCYX1454139, had significant anti-HBV activities (Fig. 6A,C). Alisporivir (Debio 025), an anti-HCV drug candidate,[38] also decreased HBV infection to the equivalent level to CsA (Fig. 6B). Figure 6D shows a dose-dependent reduction of HBs secretion by treatment with SCYX618806, SCYX827830, and SCYX1454139, all of which had more potent anti-HBV activities than CsA (compare Fig. 6D with Fig. 2A). These results indicate that anti-HBV activity is not disrupted by at least some changes to the 3-glycine, 4-leucine, and 8-alanine residues of CsA, although additional analogs will need to be evaluated for a full understanding of the structure-activity relationships. Notably, SCYX618806 and alisporivir bear modifications on the 4-leucine residue of the CsA backbone that prevent CN binding and immunosuppressive activity (Table S1), further confirming that anti-HBV activity does not require immunosuppressive activity. Notably, SCYX1454139 showed the strongest anti-HBV entry activity among 50 CsA derivatives examined (data not shown and Fig. 6E). The median inhibitory concentrations (IC_{50}s) for anti-HBV activity as well as CC_{50}s determined by an MTT-based cell viability assay are shown in Fig. 6E. The IC_{50} and CC_{50} of SCYX1454139 were 0.17 ± 0.02 and >10

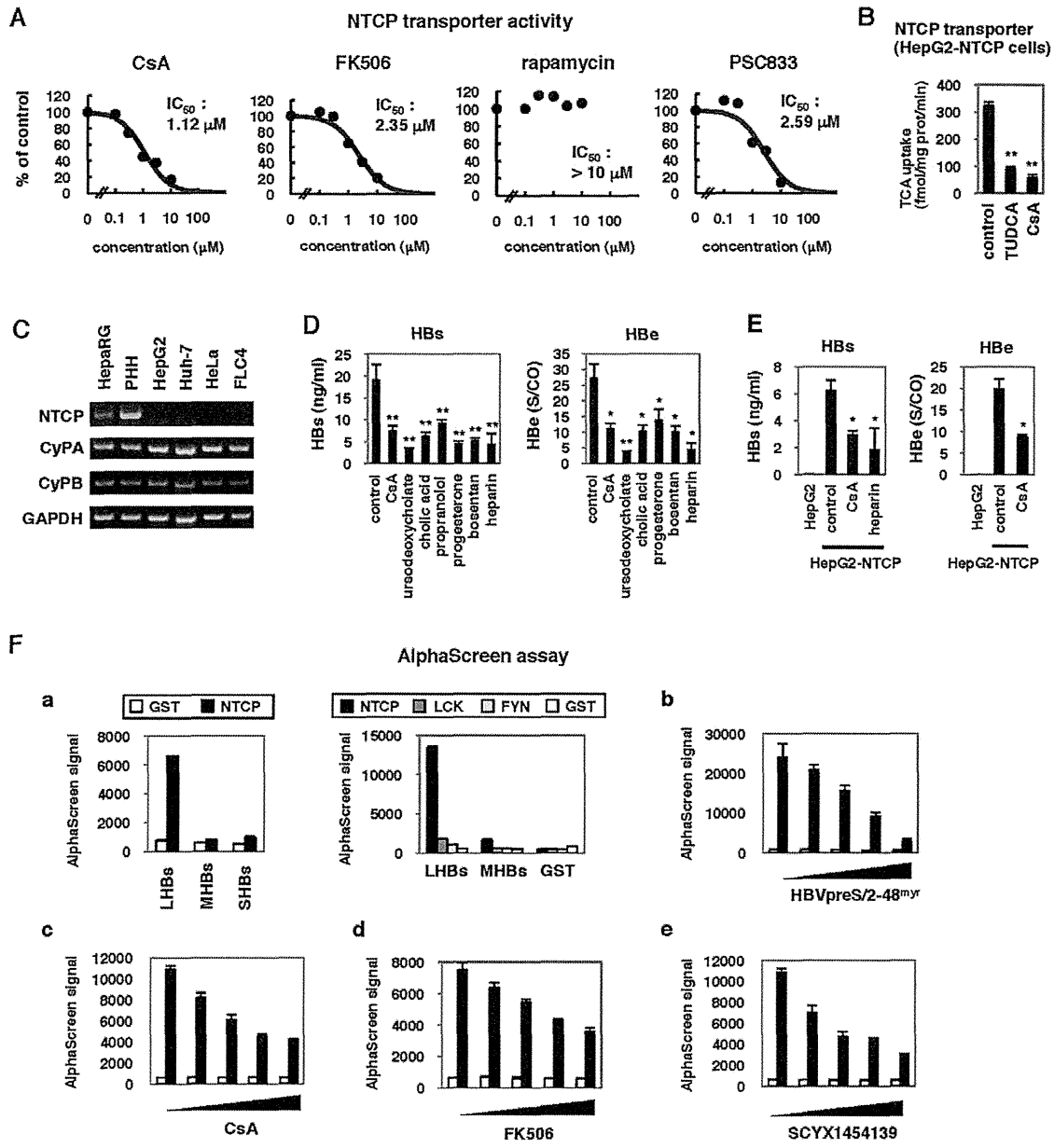

Fig. 5. NTCP inhibitors blocked HBV infection. (A) NTCP transporter activity was examined following CsA, FK506, rapamycin, and PSC833 treatment of 293 cells overexpressing NTCP, as described in the Materials and Methods. Dose-response curves and IC_{50}s for inhibition of NTCP transporter activity are shown. (B) NTCP transporter activity was measured in HepG2-NTCP cells treated with or without CsA 10 μM or tauroursodeoxycholic acid (TUDCA) 10 μM as a positive control. (C) Expression of mRNAs for NTCP, CyPA, CyPB, and GAPDH in HepaRG, PHHs, HepG2, Huh-7, HeLa, and FLC4 cells was determined by RT-PCR. (D) HepaRG cells were treated with or without CsA 4 μM, ursodeoxycholate 100 μM, cholic acid 100 μM, propranolol 100 μM, progesterone 40 μM, bosentan 100 μM, and heparin 25 U/mL according to the scheme in Fig. 1A. Secretion of HBs and HBe was quantified. (E) HepG2 cells overexpressing NTCP (HepG2-NTCP) and the parental HepG2 cells were pretreated with or without CsA or heparin for 2 hours, then treated with HBV for 16 hours. HBV infection was monitored with HBs and HBe secreted from the cells. (F) AlphaScreen assay to evaluate the binding between NTCP and large envelope protein (LHBs) as described in the Materials and Methods. (a) Left, His-tagged GST (white bars) or NTCP (black bars) are incubated with large (LHBs), middle (MHBs), or small envelope protein (SHBs). Right, His-tagged NTCP and other nonrelevant proteins, LCK and FYN, and GST were incubated with LHBs, MHBs, and GST. (b-e) His-tagged GST (white bars) or NTCP (black bars) were incubated with LHBs in the presence of varying amounts of pre-S1 lipopeptide HBVpreS/2-48^{myr} (b; 0, 7.7, 15.3, 30.7, and 61.3 μM), CsA (c; 0, 37.5, 75, 150, and 300 μM), FK506 (d; 31, 63, 125, 250, and 500 μM), and SCYX1454139 (e; 0, 37.5, 75, 150, and 300 μM), respectively. $^*P < 0.05$, $^{**}P < 0.01$.

μM, respectively, a profile superior to that of CsA (IC_{50} and CC_{50} of 1.17 ± 0.22 and >10 μM, respectively). Inhibition of HBV infection by treatment with SCYX1454139 was also observed in PHHs, in which also the anti-HBV effect of SCYX1454139 was more remarkable than that of CsA (Fig. 6F). These results

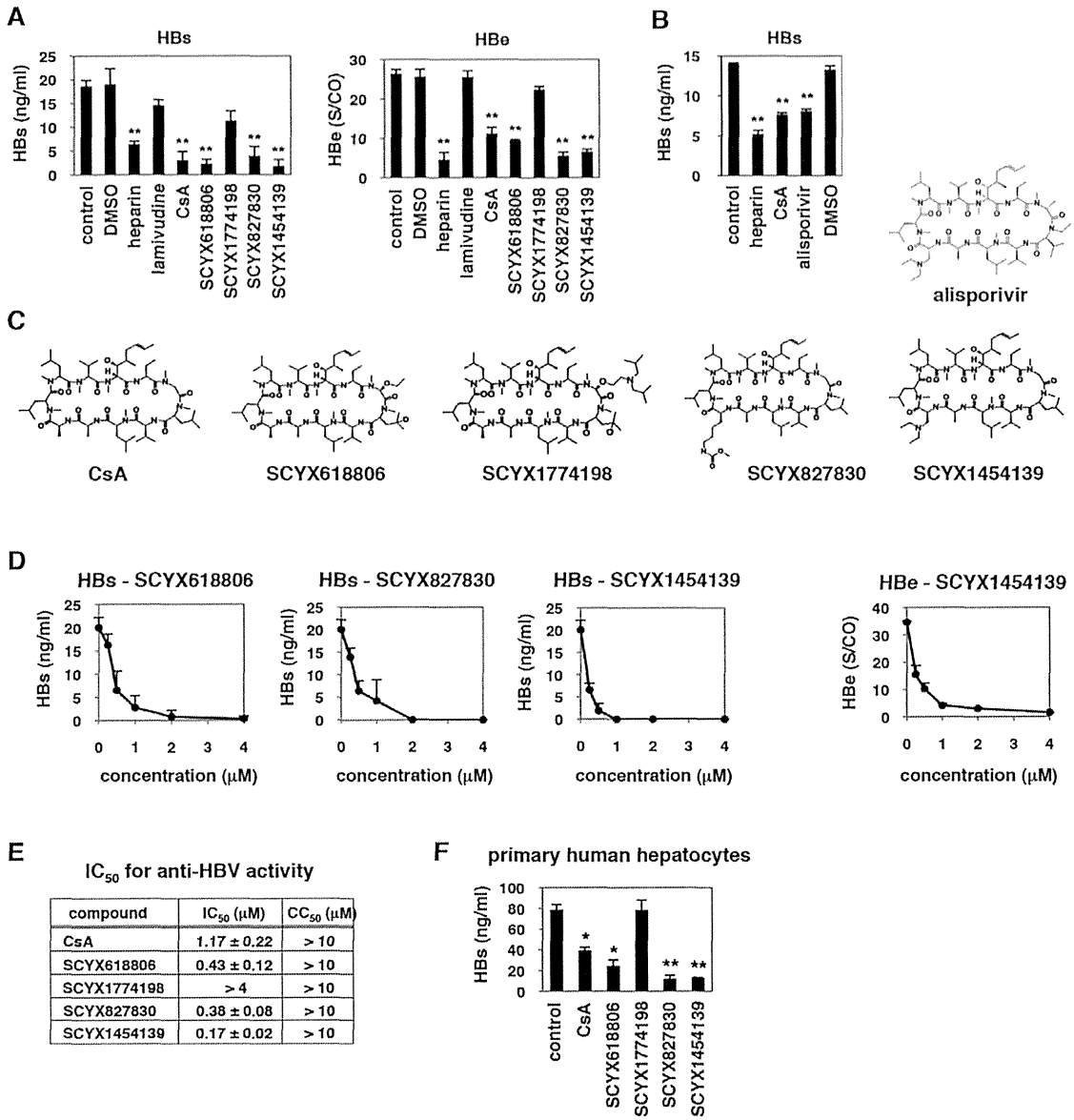

compound	IC_{50} (μM)	CC_{50} (μM)
CsA	1.17 ± 0.22	> 10
SCYX618806	0.43 ± 0.12	> 10
SCYX1774198	> 4	> 10
SCYX827830	0.38 ± 0.08	> 10
SCYX1454139	0.17 ± 0.02	> 10

Fig. 6. Analysis of CsA analogs. (A,B) Anti-HBV activity of CsA analogs. HepaRG cells were treated with or without dimethyl sulfoxide (DMSO), heparin 10 U/mL, lamivudine 1 μM, CsA 4 μM, or its analogs, SCYX618806, SCYX1774198, SCYX827830, and SCYX1454139 (A) or alisporivir (B) at 4 μM, as shown in Fig. 1A to measure HBs and HBe secretion level. (C) Chemical structures of CsA and its derivatives. (D) Dose-response curves for CsA analogs. HepaRG cells were treated with or without various concentrations of SCYX618806, SCYX827830, or SCYX1454139 (0.25, 0.5, 1, 2, and 4 μM) as shown in Fig. 1A. (E) IC_{50}s (μM) for CsA and its analogs in blocking HBV infection are shown. CC_{50}s (μM) determined by the MTT cell viability assay are also shown. (F) PHHs were treated with CsA and its derivatives at 4 μM or left untreated according to the protocol in Fig. 1A, and HBV infection was monitored by HBs protein secretion. $^{*}P < 0.05$, $^{**}P < 0.01$.

clearly indicate that analogs of CsA may include compounds with greater anti-HBV potency than that of CsA itself.

Discussion

Previous reports have demonstrated that CsA suppresses the replication of a variety of viruses including human immunodeficiency virus, HCV, influenza virus, severe acute respiratory syndrome coronavirus, human papillomavirus, flaviviruses, vesicular stomatitis virus, and vaccinia virus.[16,39-46] Virological analyses using CsA further demonstrate that CyPs are involved in the replication of these viruses. In this study, we showed that CsA inhibited the entry of HBV but in an apparent CyP-independent manner. It was previously reported that CsA suppressed HBV replication in a cell culture system carrying an HBV transgene.[47] However,

this antireplication effect is not likely to be responsible for the anti-HBV activity observed in this study, based on several observations. First, the experimental system mainly used in this study (Fig. 1A) is likely to evaluate the early phase of HBV infection but not HBV replication. Second, the suppression of HBV replication by CsA reported previously was mediated by blocking the mitochondrial permeability transition pore possibly through binding to mitochondrial CyPD.[47,48] The anti-HBV activity shown in this study, however, had no correlation with binding to CyPs, suggesting that the inhibition of HBV infection in HepaRG cells and PHHs is not from the result of suppression of HBV replication. Rather, CsA inhibited NTCP transporter activity and disrupted the binding between NTCP and LHBs *in vitro*. Moreover, inhibition of HBV infection could be observed by treatment with other compounds having the capacity to inhibit NTCP. These results suggest that targeting NTCP blocks HBV infection.

The current anti-HBV agents are mainly comprised of nucleos(t)ide analogs and IFNs. Development of anti-HBV agents targeting different molecules is greatly needed for achieving improved treatment of HBV infection, especially to combat drug-resistant virus. HBV cell entry mechanisms have been poorly defined. At the initial stage, HBV attaches to target cells with low affinity through binding involving cellular factors including heparan sulfate proteoglycans.[28,29] For the subsequent entry mechanism, it has recently been reported that NTCP is essential for HBV-specific entry.[22] Although the precise mechanism for entry and internalization is as yet incompletely understood, interference with this step has emerged as an attractive approach for development of novel therapeutics. For example, Gripon et al.[5] demonstrated that a peptide mimicking the pre-S1 region of large envelope protein prevented HBV infection in a mouse model. These results suggest that inhibition of virus cell entry could be an effective strategy for preventing HBV infection to achieve clinical outcomes such as for postexposure prophylaxis, blockage of vertical transmission, and prevention of HBV recurrence after liver transplantation. Given that HBV reactivation generally occurs under immunosuppressive conditions,[49,50] it is uncertain whether clinically relevant doses of CsA or FK506 could be helpful in preventing HBV reactivation after liver transplantation. It remains also unknown in general whether entry inhibitors could be effective in eliminating chronic HBV infection. Future studies should evaluate whether inhibition of HBV entry by CsA or its derivatives can reduce persistent HBV infection, especially in combination with nucleos(t)ide analogs or interferons. In this study, we obtained nonimmunosuppressive CsA derivatives that could inhibit HBV entry (Fig. 6). Moreover, a small-scale analog analysis identified a CsA derivative exhibiting more potent inhibition of HBV infection, with an IC_{50} of 0.1-0.2 μM (Fig. 6). This IC_{50} is equivalent to the anti-HCV replication activities of alisporivir or SCY-635 (0.22 μM and 0.08 μM, respectively), drugs which have been shown to reduce HCV viral load in infected patients during clinical trials.[38] Further analog analysis using CsA as a platform may identify more potent anti-HBV compounds.

In general, antiviral drugs targeting a cellular factor select drug-resistant viruses at a lower frequency than do direct-acting antiviral agents. Cellular targets relevant for anti-HBV drug development have been poorly defined to date. This study has demonstrated that small molecules targeting NTCP can inhibit HBV infection. Further study of NTCP inhibitors and CsA derivatives may provide a new anti-HBV strategy targeting a cellular factor, which is less likely to foster emergence of drug-resistant viruses.

Acknowledgment: HepAD38 and Huh-7.5.1 cells were kindly provided by Dr. Christoph Seeger at Fox Chase Cancer Center and Dr. Francis Chisari at Scripps Research Institute. Purified CyPA, B, and D were generous gifts from Dr. Gunter Fischer, Max Planck Research Unit for Enzymology of Protein Folding, Halle, Germany. Plasmids for the HCVpp system were the kind gift from Dr. Francois-Loic Cosset at the University of Lyon. A pre-S1 lipopeptide HBVpreS/2-48^{myr} was kindly provided by Dr. Stephan Urban at the University Hospital Heidelberg. We are also grateful to all of the members of Department of Virology II, National Institute of Infectious Diseases.

References

1. Pawlotsky JM, Dusheiko G, Hatzakis A, Lau D, Lau G, Liang TJ, et al. Virologic monitoring of hepatitis B virus therapy in clinical trials and practice: recommendations for a standardized approach. Gastroenterology 2008;134:405-415.
2. Rapicetta M, Ferrari C, Levrero M. Viral determinants and host immune responses in the pathogenesis of HBV infection. J Med Virol 2002;67:454-457.
3. Zoulim F. Hepatitis B virus resistance to antiviral drugs: where are we going? Liver Int 2011;31(Suppl 1):111-116.
4. Grimm D, Thimme R, Blum HE. HBV life cycle and novel drug targets. Hepatol Int 2011;5:644-653.
5. Gripon P, Cannie I, Urban S. Efficient inhibition of hepatitis B virus infection by acylated peptides derived from the large viral surface protein. J Virol 2005;79:1613-1622.
6. Petersen J, Dandri M, Mier W, Lutgehetmann M, Volz T, von Weizsacker F, et al. Prevention of hepatitis B virus infection in vivo by entry inhibitors derived from the large envelope protein. Nat Biotechnol 2008;26:335-341.

7. Delaney WEt, Edwards R, Colledge D, Shaw T, Furman P, Painter G, et al. Phenylpropenamide derivatives AT-61 and AT-130 inhibit replication of wild-type and lamivudine-resistant strains of hepatitis B virus in vitro. Antimicrob Agents Chemother 2002;46:3057-3060.
8. Deres K, Schroder CH, Paessens A, Goldmann S, Hacker HJ, Weber O, et al. Inhibition of hepatitis B virus replication by drug-induced depletion of nucleocapsids. Science 2003;299:893-896.
9. King RW, Ladner SK, Miller TJ, Zaifert K, Perni RB, Conway SC, et al. Inhibition of human hepatitis B virus replication by AT-61, a phenylpropenamide derivative, alone and in combination with (-)beta-L-2',3'-dideoxy-3'-thiacytidine. Antimicrob Agents Chemother 1998; 42:3179-3186.
10. Weber O, Schlemmer KH, Hartmann E, Hagelschuer I, Paessens A, Graef E, et al. Inhibition of human hepatitis B virus (HBV) by a novel non-nucleosidic compound in a transgenic mouse model. Antiviral Res 2002;54:69-78.
11. Block TM, Lu X, Mehta AS, Blumberg BS, Tennant B, Ebling M, et al. Treatment of chronic hepadnavirus infection in a woodchuck animal model with an inhibitor of protein folding and trafficking. Nat Med 1998;4:610-614.
12. Block TM, Lu X, Platt FM, Foster GR, Gerlich WH, Blumberg BS, et al. Secretion of human hepatitis B virus is inhibited by the imino sugar N-butyldeoxynojirimycin. Proc Natl Acad Sci U S A 1994;91: 2235-2239.
13. Watashi K, Shimotohno K. Cyclophilin and viruses: cyclophilin as a cofactor for viral infection and possible anti-viral target. Drug Target Insights 2007;2:9-18.
14. Loor F, Tiberghien F, Wenandy T, Didier A, Traber R. Cyclosporins: structure-activity relationships for the inhibition of the human MDR1 P-glycoprotein ABC transporter. J Med Chem 2002;45:4598-4612.
15. El-Farrash MA, Aly HH, Watashi K, Hijikata M, Egawa H, Shimotohno K. In vitro infection of immortalized primary hepatocytes by HCV genotype 4a and inhibition of virus replication by cyclosporin. Microbiol Immunol 2007;51:127-133.
16. Watashi K, Hijikata M, Hosaka M, Yamaji M, Shimotohno K. Cyclosporin A suppresses replication of hepatitis C virus genome in cultured hepatocytes. HEPATOLOGY 2003;38:1282-1288.
17. Nakagawa M, Sakamoto N, Tanabe Y, Koyama T, Itsui Y, Takeda Y, et al. Suppression of hepatitis C virus replication by cyclosporin a is mediated by blockade of cyclophilins. Gastroenterology 2005;129: 1031-1041.
18. Watashi K, Ishii N, Hijikata M, Inoue D, Murata T, Miyanari Y, et al. Cyclophilin B is a functional regulator of hepatitis C virus RNA polymerase. Mol Cell 2005;19:111-122.
19. Yang F, Robotham JM, Nelson HB, Irsigler A, Kenworthy R, Tang H. Cyclophilin A is an essential cofactor for hepatitis C virus infection and the principal mediator of cyclosporine resistance in vitro. J Virol 2008;82:5269-5278.
20. Schlutter J. Therapeutics: new drugs hit the target. Nature 2011;474: S5-S7.
21. Watashi K. Alisporivir, a cyclosporin derivative that selectively inhibits cyclophilin, for the treatment of HCV infection. Curr Opin Investig Drugs 2010;11:213-224.
22. Yan H, Zhong G, Xu G, He W, Jing Z, Gao Z, et al. Sodium taurocholate cotransporting polypeptide is a functional receptor for human hepatitis B and D virus. Elife 2012;1:e00049.
23. Watashi K, Liang G, Iwamoto M, Marusawa H, Uchida N, Daito T, et al. Interleukin-1 and tumor necrosis factor-alpha trigger restriction of hepatitis b virus infection via a cytidine deaminase activation-induced cytidine deaminase (AID). J Biol Chem 2013;288:31715-31727.
24. Nakajima S, Watashi K, Kamisuki S, Tsukuda S, Takemoto K, Matsuda M, et al. Specific inhibition of hepatitis C virus entry into host hepatocytes by fungi-derived sulochrin and its derivatives. Biochem Biophys Res Commun 2013;440:515-520.
25. Mita S, Suzuki H, Akita H, Hayashi H, Onuki R, Hofmann AF, et al. Inhibition of bile acid transport across Na+/taurocholate cotransporting polypeptide (SLC10A1) and bile salt export pump (ABCB 11)-coexpressing LLC-PK1 cells by cholestasis-inducing drugs. Drug Metab Dispos 2006;34:1575-1581.
26. Takai K, Sawasaki T, Endo Y. Practical cell-free protein synthesis system using purified wheat embryos. Nat Protoc 2010;5:227-238.
27. Gripon P, Rumin S, Urban S, Le Seyec J, Glaise D, Cannie I, et al. Infection of a human hepatoma cell line by hepatitis B virus. Proc Natl Acad Sci U S A 2002;99:15655-15660.
28. Leistner CM, Gruen-Bernhard S, Glebe D. Role of glycosaminoglycans for binding and infection of hepatitis B virus. Cell Microbiol 2008;10: 122-133.
29. Schulze A, Gripon P, Urban S. Hepatitis B virus infection initiates with a large surface protein-dependent binding to heparan sulfate proteoglycans. HEPATOLOGY 2007;46:1759-1768.
30. Funk A, Mhamdi M, Hohenberg H, Will H, Sirma H. pH-independent entry and sequential endosomal sorting are major determinants of hepadnaviral infection in primary hepatocytes. HEPATOLOGY 2006;44:685-693.
31. De Clercq E, Ferir G, Kaptein S, Neyts J. Antiviral treatment of chronic hepatitis B virus (HBV) infections. Viruses 2010;2:1279-1305.
32. Locarnini S, Zoulim F. Molecular genetics of HBV infection. Antivir Ther 2010;15(Suppl 3):3-14.
33. Ladner SK, Otto MJ, Barker CS, Zaifert K, Wang GH, Guo JT, et al. Inducible expression of human hepatitis B virus (HBV) in stably transfected hepatoblastoma cells: a novel system for screening potential inhibitors of HBV replication. Antimicrob Agents Chemother 1997;41: 1715-1720.
34. Aizaki H, Morikawa K, Fukasawa M, Hara H, Inoue Y, Tani H, et al. Critical role of virion-associated cholesterol and sphingolipid in hepatitis C virus infection. J Virol 2008;82:5715-5724.
35. Kim RB, Leake B, Cvetkovic M, Roden MM, Nadeau J, Walubo A, et al. Modulation by drugs of human hepatic sodium-dependent bile acid transporter (sodium taurocholate cotransporting polypeptide) activity. J Pharmacol Exp Ther 1999;291:1204-1209.
36. Leslie EM, Watkins PB, Kim RB, Brouwer KL. Differential inhibition of rat and human Na+-dependent taurocholate cotransporting polypeptide (NTCP/SLC10A1)by bosentan: a mechanism for species differences in hepatotoxicity. J Pharmacol Exp Ther 2007;321:1170-1178.
37. Palacios EH, Weiss A. Function of the Src-family kinases, Lck and Fyn, in T-cell development and activation. Oncogene 2004;23:7990-8000.
38. Paeshuyse J, Kaul A, De Clercq E, Rosenwirth B, Dumont JM, Scalfaro P, et al. The non-immunosuppressive cyclosporin DEBIO-025 is a potent inhibitor of hepatitis C virus replication in vitro. HEPATOLOGY 2006;43:761-770.
39. Bienkowska-Haba M, Patel HD, Sapp M. Target cell cyclophilins facilitate human papillomavirus type 16 infection. PLoS Pathog 2009;5: e1000524.
40. Bose S, Mathur M, Bates P, Joshi N, Banerjee AK. Requirement for cyclophilin A for the replication of vesicular stomatitis virus New Jersey serotype. J Gen Virol 2003;84:1687-1699.
41. Damaso CR, Moussatche N. Inhibition of vaccinia virus replication by cyclosporin A analogues correlates with their affinity for cellular cyclophilins. J Gen Virol 1998;79(Pt 2):339-346.
42. Liu X, Zhao Z, Li Z, Xu C, Sun L, Chen J, et al. Cyclosporin A inhibits the influenza virus replication through cyclophilin A-dependent and -independent pathways. PLoS One 2012;7:e37277.
43. Luban J, Bossolt KL, Franke EK, Kalpana GV, Goff SP. Human immunodeficiency virus type 1 Gag protein binds to cyclophilins A and B. Cell 1993;73:1067-1078.
44. Pfefferle S, Schopf J, Kogl M, Friedel CC, Muller MA, Carbajo-Lozoya J, et al. The SARS-coronavirus-host interactome: identification of cyclophilins as target for pan-coronavirus inhibitors. PLoS Pathog 2011;7:e1002331.
45. Qing M, Yang F, Zhang B, Zou G, Robida JM, Yuan Z, et al. Cyclosporine inhibits flavivirus replication through blocking the interaction between host cyclophilins and viral NS5 protein. Antimicrob Agents Chemother 2009;53:3226-3235.

46. Towers GJ, Hatziioannou T, Cowan S, Goff SP, Luban J, Bieniasz PD. Cyclophilin A modulates the sensitivity of HIV-1 to host restriction factors. Nat Med 2003;9:1138-1143.
47. Bouchard MJ, Puro RJ, Wang L, Schneider RJ. Activation and inhibition of cellular calcium and tyrosine kinase signaling pathways identify targets of the HBx protein involved in hepatitis B virus replication. J Virol 2003;77:7713-7719.
48. Xia WL, Shen Y, Zheng SS. Inhibitory effect of cyclosporine A on hepatitis B virus replication in vitro and its possible mechanisms. Hepatobil Pancreat Dis Int 2005;4:18-22.
49. Coffin CS, Terrault NA. Management of hepatitis B in liver transplant recipients. J Viral Hepat 2007;14(Suppl 1):37-44.
50. Fox AN, Terrault NA. The option of HBIG-free prophylaxis against recurrent HBV. J Hepatol 2012;56:1189-1197.

Table 1. Sorafenib-Related Adverse Events (AEs)

Toxicity	Grade 1	Grade 2	Grade 3	Total
Nonhematological				
HFS	6 (19.3%)	3 (9.7%)	6 (19.3%)	15 (48.4%)
Diarrhea	7 (22.6%)	6 (19.3%)	1 (3.2%)	14 (45.2%)
Abdominal pain	7 (22.6%)	1 (3.2%)	3 (9.7%)	11 (35.5%)
Fatigue	7 (22.6%)	10 (32.2%)	7 (22.6%)	24 (77.4%)
Anorexia	0 (0%)	9 (29.0%)	0 (0%)	9 (29.0%)
Nausea	4 (12.9%)	1 (3.2%)	0 (0%)	5 (16.1%)
Hyperbilirubinemia	9 (29.0%)	3 (9.7%)	3 (9.7%)	15 (48.4%)
Hypertransaminasemia	18 (58.1%)	6 (19.3%)	0 (0%)	24 (77.4%)
Hematological				
Thrombocytopenia	13 (41.9%)	3 (9.7%)	4 (12.9%)	20 (64.5%)
Neutropenia	1 (3.2%)	4 (12.9%)	0 (0%)	5 (16.1%)
Anemia	1 (3.2%)	3 (9.7%)	0 (0%)	4 (12.9%)

Therefore, we conducted a retrospective analysis to evaluate the tolerability of sorafenib in elderly patients with advanced HCC. The study involved a consecutive cohort of 31 patients, aged between 70 and 83 years, with advanced HCC, Child-Pugh A or B, Eastern Cooperative Oncology Group (ECOG) Performance Status 0-2, and who were not suitable candidates for or had progressed after locoregional therapies. Patients were treated with single-agent sorafenib, at a standard dose of 400 mg twice daily orally. Treatment was continued until disease progression or unacceptable toxicity. Self-sufficiency and impact of treatment on quality of life were assessed administering the IADL (Instrumental Activities of Daily Living) scale at baseline and every clinic visit. Adverse events (AEs) were reported using the National Cancer Institute Common Terminology Criteria for Adverse Events (NCI CTCAE) version 3.0.

Our sample included an elderly population with frequent comorbidities. The most represented (80.6%) were cardiovascular diseases (primarily hypertension). Therefore, blood pressure was monitored weekly during the first 6 weeks of treatment and regularly thereafter. No adjustment or new institution of antihypertensive therapy was required. The median duration of sorafenib treatment was 139 days, ranging from a minimum of 1 to a maximum of 12 months. AEs were reported in all patients, mostly during the first month and of grade 1 or 2. Grade 3 side effects were fatigue (22.6%), hand-foot syndrome (19.3%), thrombocytopenia (12.9%), hyperbilirubinemia (9.7%), abdominal pain (9.7%), and, only in one case, diarrhea (3.2%). No grade 4 toxicity was noted (Table 1). At baseline, the IADL score was >5 in 22 (71%) patients. Only 150 days after starting treatment, that IADL score decreased in 6 (19.3%) of 21 patients. This proves that the observed toxicity did not affect the quality of life and the level of self-sufficiency of most patients.

Our results indicate that sorafenib therapy is well tolerated also in elderly patients with advanced HCC and it has a positive impact on their self-sufficiency and quality of life.

Given the retrospective nature and the small sample size of this analysis, our conclusions could be considered not generalizable. However, we hope that they will prompt future prospective studies which will focus more on the HCC elderly population.

EDOARDO FRANCINI, M.D.
VINCENZO BIANCO, M.D.
Sapienza University of Rome
Medical Oncology Unit
Rome, Italy

Reference

1. Jemal A, Siegel R, Xu J, Ward E. Cancer statistics, 2010. CA Cancer J Clin 2010;60:277-300.

View this article online at wileyonlinelibrary.com.
DOI 10.1002/hep.26921
Potential conflict of interest: Nothing to report.

Strategy for Preventing Hepatitis B Reactivation in Patients With Resolved Hepatitis B Virus Infection After Rituximab-Containing Chemotherapy

To the Editor:

In a recent article in HEPATOLOGY, Hsu et al.[1] reported on a prospective study (NCT00931299) to determine the incidence of hepatitis B virus (HBV) reactivation in 150 patients with resolved HBV infection receiving rituximab/CHOP chemotherapy. The researchers indicated that HBV reactivation is not uncommon and can be managed with regular monitoring of HBV DNA in serum. However, there are some concerns regarding the management of HBV DNA monitoring as described in this report.

First, Hsu et al.[1] reported that no HBV-related death occurred during the study period, but that HBV-related severe hepatitis and chemotherapy delay occurred in 7 (4.6%) and 2 (1.3%) patients, respectively. Furthermore, patients with HBV reactivation may have a poorer prognosis than those without reactivation, suggesting that HBV DNA monitoring could not enable successful management of HBV reactivation in this setting. In fact, the researchers have already described the usefulness of a more-sensitive HBV DNA assay and they should show whether a second polymerase chain reaction assay (detection limit: 300 copies/mL, assay #2) could prevent severe hepatitis flare resulting from HBV reactivation by estimating, in their retrospective analysis, the exact time between early HBV DNA detection and onset of hepatitis.

Second, Hsu et al.[1] concluded that reappearance of hepatitis B surface antigen (HBsAg) was the most important predictor of HBV-related hepatitis flare, but there is no information regarding the sensitivity and specificity of the HBsAg assay and these might influence clinical outcome. The researchers should provide information regarding the HBsAg assay in the Methods section and specify the time between the reappearance of HBsAg and onset of HBV-related hepatitis. In addition, they should specify the incidence of reappearance of HBsAg with persistence for more than 6 months in patients with HBV reactivation, because the chronic HBV carrier state might negatively influence long-term outcomes, regardless of fulminant hepatitis and HBV-related death.

Third, Hsu et al.[1] discussed the importance of host factors associated with HBV reactivation, but several articles have reported that the development of fulminant hepatitis was associated with viral factors, which especially included high levels of replication associated with mutations in the precore region.[2,3] The researchers should specify whether the kinetics of HBV DNA and severe hepatitis were associated with precore and/or basal core promoter mutations in the patients with HBV reactivation, because general readers need to be aware of such important viral factors to perform safe monitoring of HBV DNA.

Preemptive antiviral therapy guided by regular monitoring of HBV DNA is a reasonable strategy to prevent HBV reactivation

in patients with resolved HBV infection,[1,4,5] but a standard management according to the risk of HBV reactivation has not been established as yet. We hope that the additional information can help readers regarding the optimal interval and sensitivity of the HBV DNA monitoring assay. In addition, if the reappearance of HBsAg and viral mutations related to viral replication are good predictive markers for severe hepatitis resulting from HBV reactivation, we can recommend that antiviral treatment should be started immediately for those patients with HBV reactivation.

SHIGERU KUSUMOTO, M.D., PH.D.[1]
YASUHITO TANAKA, M.D., PH.D.[2]
MASASHI MIZOKAMI, M.D., PH.D.[3]
RYUZO UEDA, M.D., PH.D.[4]
[1]Department of Medical Oncology and Immunology
Nagoya City University Graduate School of Medical Sciences
Nagoya, Japan
[2]Department of Virology and Liver Unit
Nagoya City University Graduate School of Medical Sciences
Nagoya, Japan
[3]The Research Center for Hepatitis and Immunology
National Center for Global Health and Medicine
Ichikawa, Japan
[4]Department of Tumor Immunology
Aichi Medical University School of Medicine
Aichi, Japan

References

1. Hsu C, Tsou HH, Lin SJ, Wang MC, Yao M, Hwang WL, et al. Chemotherapy-induced hepatitis B reactivation in lymphoma patients with resolved HBV infection: a prospective study. HEPATOLOGY 2014;59:2092-2100.
2. Omata M, Ehata T, Yokosuka O, Hosoda K, Ohto M. Mutations in the precore region of hepatitis B virus DNA in patients with fulminant and severe hepatitis. N Engl J Med 1991;324:1699-1704.
3. Ozasa A, Tanaka Y, Orito E, Sugiyama M, Kang JH, Hige S, et al. Influence of genotypes and precore mutations on fulminant or chronic outcome of acute hepatitis B virus infection. HEPATOLOGY 2006;44:326-334.
4. Oketani M, Ido A, Uto H, Tsubouchi H. Prevention of hepatitis B virus reactivation in patients receiving immunosuppressive therapy or chemotherapy. Hepatol Res 2012;42:627-636.
5. European Association for the Study of the Liver et al. EASL clinical practice guidelines: management of chronic hepatitis B virus infection. J Hepatol 2012;57:167-185.

View this article online at wileyonlinelibrary.com.
DOI 10.1002/hep.26963
Potential conflict of interest: Dr. Kusumoto has received research funding from Chugai Pharmaceutical Co. Ltd. and honoraria from Chugai Pharmaceutical Co. Ltd., Bristol-Myers Squibb, Zenyaku Kogyo, and Abbott. He is on the speakers' bureau for Chugai, Abbott, Zenyaku Kogyu, and Bristol-Myers Squibb. Dr. Tanaka has received research funding from Chugai Pharmaceutical Co. Ltd. and Bristol-Myers Squibb and has received honoraria from Chugai Pharmaceutical Co. Ltd., Bristol-Myers Squibb, Zenyaku Kogyo, and Abbott. He is on the speakers' bureau for Bristol-Myers Squibb, Chugai, Abbott, and Zenyaku Kogyo. Dr. Mizokami has received honoraria from and is on the speakers' bureau for Chugai Pharmaceutical Co. Ltd. and Abbott. Dr. Ueda has received research funding from Chugai Pharmaceutical Co. Ltd. and Kyowa Hakko Kirin Co. Ltd.

Reply:

We thank Dr. Kusumoto and his colleagues for their comments on our study.[1] Management of chemotherapy-induced hepatitis B virus (HBV) reactivation in lymphoma patients with resolved HBV infection is a challenging issue in endemic areas because 50%-60% of the general population in those areas have resolved HBV infection, and the clinical courses of HBV reactivation in this patient population vary greatly. Dr. Kusumoto pointed out several important points that warrant further investigation.

With increasing sensitivity of the HBV DNA tests, chemotherapy-induced HBV reactivation can be detected in about 20% of lymphoma patients who receive rituximab/CHOP chemotherapy and can be detected earlier (median, 11.8 weeks earlier than the less-sensitive assay).[1,2] However, in our study, most of the additional HBV reactivations detected by the more-sensitive assay were asymptomatic. Only 1 patient had a hepatitis flare, which resolved spontaneously. It is difficult to analyze whether earlier use of antiviral therapy by a more-sensitive assay can further reduce the number of HBV-related hepatitis flares, given the small number of patients. Therefore, the clinical benefit of HBV reactivation detected by the more-sensitive assay for pre-emptive antivirals remains to be established.

Reappearance of hepatitis B surface antigen (HBsAg), which can be measured conveniently in the clinic by chemiluminescent immunoassay, such as the Abbott Architect assay (Abbott Laboratories, Abbott Park, IL), was found, in our study, to be significantly associated with HBV-related hepatitis flares. The sensitivity of HBsAg tests currently used in the clinic can be as low as 0.05 IU/mL. Most of the patients were found to be $HBsAg^+$ at the time of hepatitis flare. Therefore an assay for HBsAg during the chemotherapy course is strongly advocated, in addition to HBV DNA. Whether HBsAg assay is useful, and more cost-effective for managing HBV reactivations in lymphoma patients, warrants a prospective study. Finally, we agree with Dr. Kusumoto that persistence of HBsAg positivity for more than 6 months may negatively influence long-term outcome, and long-term follow-up of patients with reappearance of HBsAg is ongoing.

Dr. Kusumoto pointed out the potential importance of viral factors, including the HBV replication levels and the presence of precore/basal core promoter mutations, in the development of severe hepatitis flare. Because the majority of the patients did not have detectable HBV DNA at baseline, we could not study the viral factors before therapy. For those patients with HBV reactivations, we are currently characterizing the viral genotypes and variants. However, because the patient number is still limited, studies of larger sample size and more-comprehensive evaluation of the viral and host factors that may contribute to HBV reactivation are definitely needed.

Dr. Huang and his colleagues recently reported on a randomized trial of prophylactic antiviral therapy in lymphoma patients with resolved HBV infection.[2] Although the short-term efficacy in preventing HBV viral reactivation was clearly demonstrated, future studies are warranted to evaluate the optimal duration of antiviral therapy, the high-risk patient population for whom prophylactic antiviral therapy is most indicated, and the effect of prophylactic antiviral therapy on long-term outcome. In the endemic area, the management strategies have to take additional factors, especially cost-effectiveness, into account.

CHIUN HSU, M.D., PH.D.[1,4]
PEI-JER CHEN, M.D., PH.D.[2,3]
ANN-LII CHENG, M.D., PH.D.[1,4]
Departments of [1]Oncology and [2]Internal Medicine
National Taiwan University Hospital
Taipei, Taiwan

Journal of Controlled Release 201 (2015) 41–48

Contents lists available at ScienceDirect

Journal of Controlled Release

journal homepage: www.elsevier.com/locate/jconrel

Treatment of neurological disorders by introducing mRNA in vivo using polyplex nanomicelles

Miyuki Baba [a,b], Keiji Itaka [a,*], Kenji Kondo [b], Tatsuya Yamasoba [b], Kazunori Kataoka [a,c,**]

[a] Laboratory of Clinical Biotechnology, Center for Disease Biology and Integrative Medicine, Graduate School of Medicine, The University of Tokyo, 7-3-1 Hongo, Bunkyo-ku, Tokyo 113-0033, Japan
[b] Department of Otolaryngology, Head and Neck Surgery, Faculty of Medicine, The University of Tokyo, 7-3-1 Hongo, Bunkyo-ku, Tokyo 113-8655, Japan
[c] Department of Materials Engineering, Graduate School of Engineering, The University of Tokyo, 7-3-1 Hongo, Bunkyo-ku, Tokyo 113-8656, Japan

ARTICLE INFO

Article history:
Received 10 September 2014
Accepted 16 January 2015
Available online 17 January 2015

Keywords:
Messenger RNA (mRNA) administration
Neurological disorders
Olfactory dysfunction
Brain-derived neurotrophic factor (BDNF)
mRNA-based therapy

ABSTRACT

Sensory nerve disorders are difficult to cure completely considering poor nerve regeneration capacity and difficulties in accurately targeting neural tissues. Administering mRNA is a promising approach for treating neurological disorders because mRNA can provide proteins and peptides in their native forms for mature non-dividing neural cells, without the need of entering their nuclei. However, direct mRNA administration into neural tissues in vivo has been challenging due to too unstable manner of mRNA and its strong immunogenicity. Thus, using a suitable carrier is essential for effective mRNA administration. For this purpose, we established a novel carrier based on the self-assembly of polyethylene glycol (PEG)–polyamino acid block copolymer, i.e. polyplex nanomicelles. To investigate the feasibility and efficacy of mRNA administration for the treatment of sensory nerve disorders, we used a mouse model of experimentally induced olfactory dysfunction. Intranasal administration of mRNA-loaded nanomicelles provided an efficient and sustained protein expression for nearly two days in nasal tissues, particularly in the lamina propria which contains olfactory nerve fibers, with effectively regulating the immunogenicity of mRNA. Consequently, once-daily intranasal administration of brain-derived neurotrophic factor (BDNF)-expressing mRNA using polyplex nanomicelles remarkably enhanced the neurological recovery of olfactory function along with repairing the olfactory epithelium to a nearly normal architecture. To the best of our knowledge, this is the first study to show the therapeutic potential of introducing exogenous mRNA for the treatment of neurological disorders. These results indicate the feasibility and safety of using mRNA, and provide a novel strategy of mRNA-based therapy.

1. Introduction

Sensory nerve disorders are difficult to cure completely considering poor nerve regeneration capacity and difficulties in accurately targeting neural tissues. Various bioactive factors, including nerve growth factor, brain-derived neurotrophic factor (BDNF) and neurotrophin-3, have been investigated for enhancing nerve regeneration and for nerve protection [1–4]. However, administering these factors in the form of recombinant proteins or peptides involves problems of poor stability under physiological conditions and a considerably short duration of action to achieve sufficient therapeutic effects; thus, their application for treatment has been hindered.

Administering mRNA is a promising approach for treating neurological disorders because mRNA has several advantages for providing therapeutic proteins or peptides to neural tissues; for example, mRNA can be used for protein or peptide expression in their native forms at a target site [5,6]. The sustained synthesis of proteins resulting from the delivered mRNA can facilitate the synchronization between the kinetics of signal receptor expression and bioactive factor availability [7]. The combined use of two or more bioactive factors to provide better neurotrophic and neuroprotective effects is much easier than using recombinant proteins or peptides, because mRNA can be designed for the expression of any protein or peptide by simply altering the base sequence [8]. Indeed, this is also true for DNA administration, however, mRNA has a much higher potential for protein expression in neural tissues, because it can be used to produce proteins and peptides in mature non-dividing neural cells, without the need for entering their nuclei. Most importantly, the probability of mRNA randomly integrating into the genome is negligible, thus avoiding the aberrant expression of oncogenes as a result of insertional mutagenesis.

However, direct mRNA administration into neural tissues in vivo has been challenging due to two major issues: (1) introduced mRNA is often too unstable to achieve sufficient protein expression and (2) mRNA is strongly immunogenic and induces immune responses through its

* Corresponding author.
** Corresponding author at: Department of Materials Engineering, Graduate School of Engineering, The University of Tokyo, 7-3-1 Hongo, Bunkyo-ku, Tokyo 113-8656, Japan.
E-mail addresses: itaka-ort@umin.net (K. Itaka), kataoka@bmw.t.u-tokyo.ac.jp (K. Kataoka).

http://dx.doi.org/10.1016/j.jconrel.2015.01.017
0168-3659/

recognition by Toll-like receptors [6,9,10]. Thus, only a few studies have attempted in vivo mRNA administration [11–13], and even fewer have attempted targeting neural tissue.

Thus, using a suitable carrier is essential for effective mRNA administration. For this purpose, we recently established a novel carrier that was applicable for in vivo mRNA delivery based on the self-assembly of polyethylene glycol (PEG)–polyamino acid block copolymer, i.e. polyplex nanomicelles [14]. These nanomicelles have a core–shell structure surrounded by a PEG outer layer, with the inner core of a functionalized polyamino acid, poly[N′-[N-(2-aminoethyl)-2-aminoethyl] aspartamide] [PAsp(DET)] [15]. PAsp(DET) has a high capacity for enhanced endosomal escape due to pH-sensitive membrane destabilization as well as the unique characteristic of rapidly degrading into nontoxic forms under physiological conditions [16–18]. The nanomicelles [PEG-PAsp(DET) block copolymer/mRNA] were shown to be safe and stable mRNA carriers to allow in vivo mRNA introduction into the central nervous system [14] and other tissues and organs (unpublished data). In addition, they exhibited a pronounced effect for regulating immune responses that could be induced by exogenous mRNA [14]. This is likely due to the shielding effect of PEG to avoid mRNA recognition by Toll-like receptors on host immune cells.

To establish the feasibility and efficacy of mRNA administration for the treatment of sensory nerve disorders, we used a mouse model of experimentally induced olfactory dysfunction [19]. Neurogenesis occurs throughout life in the olfactory epithelium, where olfactory receptor neurons (ORNs) are continuously replaced by new ORNs [20]. During this process, neurotrophic factors such as BDNF play an important role in promoting the survival and differentiation of ORNs [21]. TrkB, a high affinity receptor for BDNF, is abundantly expressed by immature and mature ORNs and globose basal cells [22], suggesting that BDNF can likely be used as a therapeutic agent to treat pathological conditions involving ORNs.

In this study, we applied BDNF-expressing mRNA into the nasal cavity using polyplex nanomicelles. The nasal cavity is a potentially attractive target for administering therapeutic agents considering its relatively large surface area of nasal mucosa and good vascularity [23], although the abundance of RNase in nasal mucus is unfavorable for mRNA administration. However, the function of polyplex nanomicelles should be underscored for effectively introducing mRNA into neural tissues. To the best of our knowledge, this is the first study to show the therapeutic potential of introducing exogenous mRNA for the treatment of neurological disorders. The effects of BDNF-expressing mRNA on impaired olfactory sensation were investigated by comprehensive analyses, including behavioral assessments of mice and histopathological evaluations of the olfactory epithelium.

2. Materials and methods

2.1. Preparation of mRNA

mRNA was prepared by in vitro transcription (IVT) of DNA templates that were constructed by inserting a protein-expressing fragment into a pSP73 vector (Promega, Madison, WI, USA) that included a T7 promoter. The protein-expressing fragments were obtained from pDNAs encoding photinus pyralis luciferase (pGL4; Promega), *Aequorea coerulescens* GFP (AcGFP; Clontech, Mountain View, CA, USA) and BDNF (pUNO1-hBDNFa; InvivoGen, San Diego, CA, USA). pDNAs were used as a template for IVT after linearization by Nde-I. IVT was performed using an mMESSAGE mMACHINE T7 Ultra Kit (Ambion, Invitrogen, Carlsbad, CA), followed by polyadenylation using a poly(A) tailing kit (Ambion). To generate modified mRNA, modified ribonucleic acid triphosphates (5-methyl-CTP, pseudo-UTP and 2-thio-UTP; TriLink BioTechnologies, San Diego, CA) were added to the reaction solution at 20% of 5-methyl-CTP of total CTP, and 10% pseudo-UTP and 10% 2-thio-UTP of total UTP, following the procedures reported previously [11]. Prior to the administration to mice, the transcribed mRNA was purified using a QIAquick PCR purification kit (Qiagen) and analyzed for size and purity with an Agilent RNA 6000 Nano Assay on a BioAnalyzer 2100 (Agilent Technologies).

2.2. Animals

Balb/c mice (7–10 weeks old) were purchased from Charles River Laboratories (Yokohama, Japan) and maintained under specific pathogen-free conditions. Mice were kept in individually ventilated cages, on a 12 h/12 h light/dark cycle, and provided food and water ad libitum. They were intraperitoneally injected with methimazole (Sigma-Aldrich Japan, Tokyo, Japan) at 150 mg/kg body weight to cause damage to the olfactory epithelium [19]. All experiments conformed to the guidelines of the University Committee for the Use and Care of Animals, University of Tokyo and the National Institutes of Health Guide for the Care and Use of Laboratory Animals.

2.3. Preparation of polyplex nanomicelle solutions

PEG-PAsp(DET) block copolymers were synthesized as previously described [15]. PEG used in this study had a molecular weight of 12,000. The polymerization degree of the PAsp(DET) portion was determined to be 57 by ^{1}H NMR analysis. To prepare polyplex nanomicelles, PEG-PAsp(DET) polymers and mRNA were separately dissolved in 10 mM HEPES buffer. At this stage, the concentration of mRNA was set to 300 μg/ml and that of PEG-PAsp(DET) was adjusted to obtain a ratio of amino groups in polymers to phosphate in mRNA (N/P ratio) of 3.

2.4. Intranasal administration

Mice were briefly anesthetized with 2.5% isoflurane (Abbott Japan Co., Ltd., Tokyo, Japan), placed in a supine position, and instilled intranasally with 50 μl of a solution containing 10 μg mRNA using a P200 Gilson pipetman.

To note is that we used mRNA solution comprised of 10 mM HEPES buffer for intranasal administration, because the hypotonic buffer would be available for intranasal administration without causing permanent damages on the nasal membrane [24–27]. It was reported that the hypotonic formulation would exert effects to temporarily open epithelial junctions and facilitate the uptake of drugs and genes [25].

2.5. Luciferase protein expression by bioluminescence assay

D-Luciferin substrate was dissolved in PBS, and the final volume was adjusted to obtain a concentration of 15 mg/ml. Bioluminescence emissions were measured using an IVIS imaging system (Xenogen, Alameda, CA, USA) 10 min after intraperitoneally injecting 200 μl of the D-luciferin solution (3 mg/mouse). Bioluminescence signals in the nose region were analyzed by background subtraction using Living Image Software version 2.50 (Xenogen).

2.6. Real-time RT-PCR for TNF-α, IL-6, and OMP mRNA in nasal tissues

Mice were sacrificed under deep anesthesia and total RNA was extracted from the nasal mucosa using an RNeasy Fibrous Tissue Mini Kit (Qiagen, Hilden, Germany), according to the manufacturer's protocol. cDNA was synthesized using a QuantiTect Reverse Transcription Kit (Qiagen, Hilden, Germany). mRNA expression for inflammatory cytokines (TNF-α and IL-6) and olfactory marker protein (OMP) was evaluated by real-time quantitative PCR (ABI Prism 7500 Sequence Detector; Applied Biosystems, Foster City, CA, USA) using TaqMan Gene Expression Assays (Mm00443258 for TNF-α, Mm00446190_m1 for IL-6, Mm00436450_m1 for OMP and Mm00607939 for β-actin). The relative mRNA expression for target genes was normalized using β-actin mRNA expression.

2.7. Histological examination after administering GFP-expressing mRNA into the nose

Mice were sacrificed and decapitated 24 h after administering GFP-expressing mRNA. The mandibles were discarded, and the trimmed heads were skinned. Serial sections (thickness, 5 μm) at the level of the anterior end of the olfactory bulb were prepared. These sections were stained with hematoxylin and eosin (H&E).

For immunohistochemical staining, 5-μm-thick frozen sections were prepared using an adhesive film-based method [28]. These sections were incubated at room temperature (RT) for 1 h with a blocking solution (PBS containing 2% fetal bovine serum and 0.1% Tween 20) to reduce non-specific antibody binding, and then incubated overnight with a rabbit anti-GFP monoclonal antibody (1:500 in the blocking solution; Invitrogen, Carlsbad, CA, USA). After several washes in PBS, the sections were incubated for 2 h at RT with an Alexa488-conjugated secondary antibody (1:200 in the blocking solution; Invitrogen, Carlsbad, CA, USA). After more washes with PBS, the nuclei were stained with Hoechst 33342 (1:300 in the blocking solution; Dojindo, Kumamoto, Japan). The sections were then observed under an Axiovert 200 fluorescence microscope (Carl Zeiss, Jena, Germany) using a 20× EC Plan Neofuar objective (Carl Zeiss). As a negative control, the primary antibody was omitted from the reaction. There was no obvious labeling corresponding to immunostaining by the primary antibody (data not shown).

2.8. Olfactory function assessments

Buried food tests were performed as previously described, with some modifications [29]. Pieces of cheese were placed in animals' cages for at least 3 consecutive days before the test to familiarize the mice to the smell of the cheese. Mice were then individually placed in cages and deprived of food for 24 h. A small piece of cheese was buried 4 cm beneath the bedding surface in a randomly chosen corner of the cage. The time required to uncover the food, to grab or to eat it was recorded. These tests were performed 4 times at intervals of 10 min. The upper time limit to uncover the food was set at 5 min (300 s). If a mouse could not uncover the food within this time limit, the cut-off of 300 s was recorded.

2.9. Histopathological examination after inducing olfactory dysfunction and treatment with BDNF-expressing mRNA

Histopathological examinations were made by H&E staining and detecting OMP expression in the olfactory epithelium. For tissue preparation, mouse heads were fixed by immersion in 10% neutral buffered formalin (Muto Kagaku, Tokyo, Japan) at RT for 1 week, followed by decalcification in 10% ethylenediaminetetraacetic acid (EDTA, pH 7.0) at 37 °C for two weeks. After decalcification, specimens were washed, dehydrated in a graded ethanol series and embedded in paraffin. Serial sections (thickness, 5 μm) at the level of the anterior end of the olfactory bulb were prepared. These sections were then stained with H&E. For OMP immunostaining, rehydrated sections were immersed in 10 mM citrate buffer (pH 6.0; Dako Cytomation Japan, Kyoto, Japan) and autoclaved at 121 °C for 20 min for antigen retrieval. Next, the sections were incubated for 1 h with a blocking solution [PBS, pH 7.4, containing 4% fetal bovine serum (Invitrogen, Tokyo, Japan), 0.1% Triton-X 100 and 0.1% sodium azide] at RT to reduce non-specific antibody binding, and then incubated with a goat anti-OMP antibody (1:5000 in the blocking solution; Wako Chemical USA, Richmond, VA) for 1 h at RT. After several washes with PBS, the sections were incubated for 1 h at RT with an Alexa546-conjugated secondary antibody (1:400 in the blocking solution; Invitrogen, Carlsbad, CA, USA). After more washes with PBS, the sections were mounted and the nuclei were stained with ProLong Gold Antifade Reagent with DAPI (Invitrogen, Carlsbad, CA, USA).

2.10. Statistical analysis

Statistical analyses were performed using StatMate (Atoms, Tokyo, Japan). One-sample Kolmogorov–Smirnov tests were used to compare the data distributions against a normal distribution. Results are expressed as mean ± standard error of the mean (SEM). A two-tailed unpaired t-test or Mann–Whitney U-test was used for statistical comparisons. $p < 0.05$ was considered to indicate statistical significance.

3. Results

3.1. Sustained protein expression in vivo after intranasal mRNA administration using polyplex nanomicelle

After incorporation into polyplex nanomicelles, luciferase-expressing mRNA (10 μg) was intranasally administered to BALB/c mice. We then evaluated luciferase expression using an IVIS imaging system; bioluminescence could be detected in nasal tissues 4 h after the administration (Fig. 1A), lasting for up to 48 h (Fig. 1B). In contrast, almost no luciferase expression was observed after administering an equal quantity of naked mRNA (Fig. 1A, B).

Histological analysis was performed using GFP-expressing mRNA. GFP-positive staining was widely observed in the lamina propria, which contains olfactory nerve fibers and endings, and in the airway epithelial cells and the basal part of the olfactory epithelial cells (Fig. 2). However, no GFP-staining was detected in nasal septal cartilages and bones.

The induction of proinflammatory cytokine genes after the administration of luciferase-expressing mRNA was evaluated using real-time quantitative PCR (qPCR) by measuring the mRNA expression levels of genes encoding tumor necrosis factor (TNF)-α and interleukin (IL)-6 in nasal tissues (Fig. 3). At 4 h after mRNA administration using the nanomicelles, cytokine gene mRNA expression levels were increased compared with untreated control levels. However, at 24 h after administration, the expression levels had decreased to untreated control levels. In contrast, when mRNA was administered in the form of naked mRNA, the increase in cytokine gene induction was significantly higher than that using the nanomicelles, even at 24 h after the administration.

3.2. Introducing BDNF-expressing mRNA using polyplex nanomicelles promotes early recovery of olfactory function

An olfactory dysfunction was induced in wild-type BALB/c mice by intraperitoneally injecting methimazole (150 mg/kg body weight) [19]. Methimazole causes cell death and degeneration in the olfactory epithelium, which leads to a transient disturbance in olfactory sensations. These sensations spontaneously show a gradual recovery over a few weeks, although the olfactory epithelium exhibits metaplasia.

We applied BDNF-expressing mRNA using polyplex nanomicelles to treat this olfactory dysfunction. Olfactory sensations were evaluated with a buried food test to determine the amount of time required for mice to uncover food [29]. As shown in Fig. 4A, the intranasal administration of BDNF-expressing mRNA into the nose significantly promoted the recovery of olfactory sensations after Day 3, as the average time required to uncover food was remarkably shorter for mice that received BDNF-expressing mRNA in comparison with control mice that received HEPES buffer. Fig. 4B shows the percentages of mice that showed curative recovery (could uncover food within 120 s) [29]. All mice that received BDNF-expressing mRNA recovered to the curative level by Day 5, whereas the control mice that received HEPES buffer required 10 days until they all recovered to the curative level.

Histopathological examinations of the damaged olfactory epithelium on Day 1 showed that administering BDNF-expressing mRNA

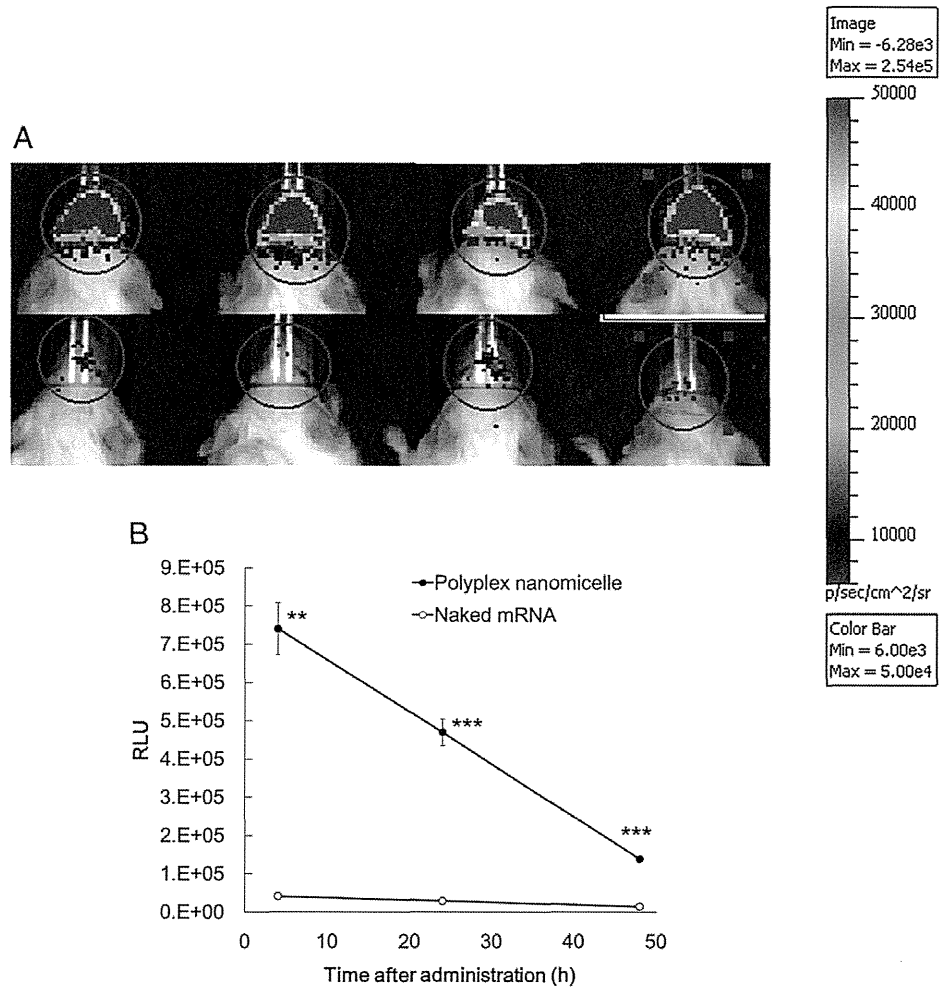

Fig. 1. Bioluminescence after intranasally administering luciferase-expressing mRNA. (A) Bioluminescence images obtained by an IVIS Imaging System 4 h after administering luciferase-expressing mRNA-loaded polyplex nanomicelles (upper) and an equal quantity of naked mRNA (lower).(B) Time course of bioluminescence after intranasally administering mRNA using polyplex nanomicelles (closed circle) and naked mRNA (open circle). Statistical analyses were performed by two-tailed Student's t-test, ***$p < 0.001$, **$p < 0.01$. RLU; relative luminescence units. Results are means ± SEMs ($n = 4$).

maintained the olfactory epithelium in a nearly-normal architecture. A gross analysis of the H&E stained sections of the nasal septa indicated that approximately half of the interior nasal surface area was covered with intact olfactory epithelium that was attached to the lamina propria (Fig. 5A). In contrast, in the control group that received HEPES buffer, the olfactory epithelium was severely sloughed (Fig. 5A) and the area covered by the intact olfactory epithelium was significantly reduced to approximately 20% (Fig. 5B).

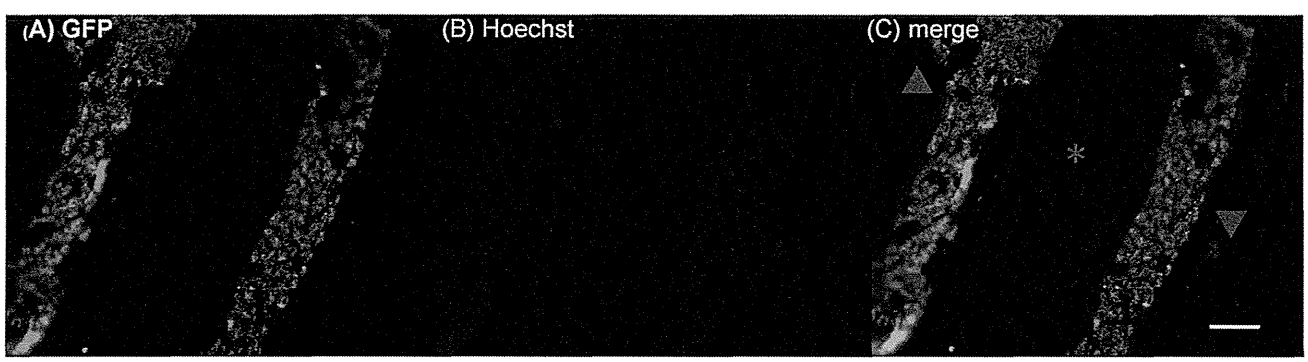

Fig. 2. Histological analysis after intranasally administering GFP-expressing mRNA. Mice were sacrificed and decapitated 24 h after administering GFP-expressing mRNA. (A) GFP expression visualized by immunostaining using an anti-GFP monoclonal antibody. (B) Cell nuclei stained by Hoechst. (C) Merged image. GFP-positive staining was widely observed in the lamina propria (arrowheads), but not in nasal septal cartilages and bones (asterisk). Scale bar: 50 μm.

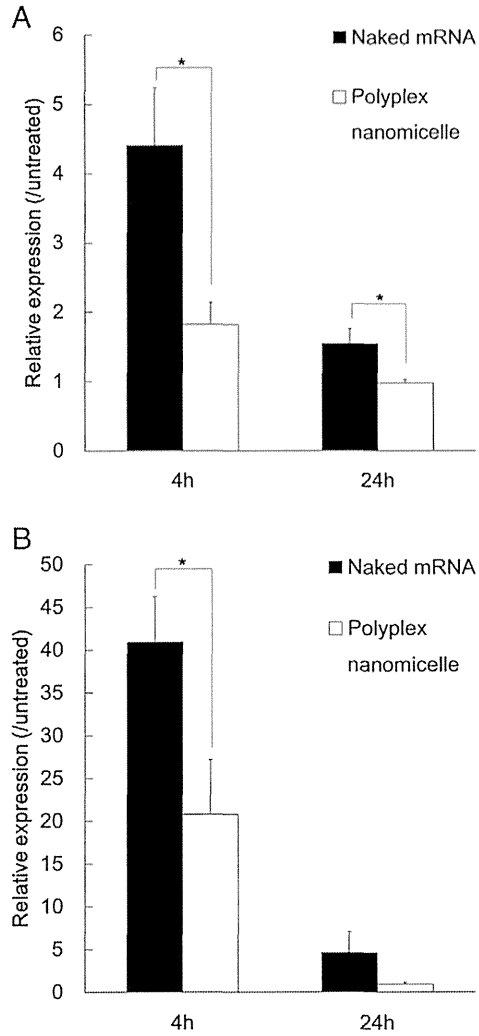

Fig. 3. Induction of proinflammatory cytokine genes after intranasal mRNA administration. Proinflammatory gene mRNA expression levels were evaluated 4 and 24 h after mRNA administration using real-time quantitative PCR (qPCR) by measuring the mRNA expression levels of genes encoding tumor necrosis factor (TNF)-α (A) and interleukin (IL)-6 (B) in nasal tissue administration of mRNA into the nasal tissue. mRNA was administered using polyplex nanomicelle (open bar) or in the form of naked mRNA (closed bar). Statistical analyses were performed by two-tailed Student's t-test, *, $p < 0.05$. Results are means ± SEMs ($n = 10$).

3.3. Introducing BDNF-expressing mRNA using polyplex nanomicelles enables complete regeneration of the olfactory epithelium after drug-induced olfactory dysfunction

To evaluate the long-term effects of BDNF-expressing mRNA on the olfactory epithelium, the thickness of the epithelium was measured via the histological sections by determining the distance between the basilar membrane and the top of the cell layer of the nasal septum. On Day 1, the group that received BDNF-expressing mRNA tended to have a thicker olfactory epithelium than the control group that received HEPES buffer (Fig. 6A, B). This was consistent with the results reported in Fig. 5 regarding the nearly normal architecture of the olfactory epithelium in the BDNF-expressing mRNA treatment group. However, on Days 4 and 7, the mean epithelial thickness was comparable between the groups, presumably due to the enhanced turnover of the epithelium [30]. Further, after Day 14, the treated group showed a higher recovery of epithelium thickness (Fig. 6A). The representative images of the histological sections suggested that the nearly normal architecture of the olfactory epithelium was recovered in the treatment group, whereas in the control group, the epithelium still showed abnormal metaplasia (Fig. 6B).

To further confirm the recovery of the olfactory epithelium after administering BDNF-expressing mRNA, we evaluated olfactory marker protein (OMP) which is specifically expressed by mature olfactory neurons [31]. By qPCR analysis of OMP mRNA expression levels in nasal tissues, OMP expression was found to be enhanced, particularly after Day 15, in the treatment group (Fig. 6C). Immunostained sections using an anti-OMP antibody (Day 28) indicated that in the treatment group, OMP-positive olfactory neurons were uniformly distributed throughout the nearly normal architecture of the olfactory epithelium (Fig. 6D), whereas in the control group, there were much fewer OMP-positive neurons and they exhibited morphological abnormalities (Fig. 6D). These results strongly suggest that BDNF-expressing mRNA effectively provided a favorable environment to enhance the regeneration of olfactory neurons.

4. Discussion

In this study, we demonstrated that intranasal mRNA administration can be used to treat an olfactory nerve dysfunction. The incorporation of mRNA into polyplex nanomicelles provided diffuse protein expression in the lamina propria. BDNF-expressing mRNA remarkably enhanced the neurological recovery from olfactory dysfunction by repairing the olfactory epithelium to a nearly normal architecture. These results clearly indicate the therapeutic potential of mRNA for neurogenic disorders via sufficient and sustained expression of therapeutic proteins or peptides.

The chief advantage of using mRNA is its competency with non-dividing cells. It is usually difficult to use pDNA transfection for non-dividing cells because of the low efficiency of nuclear import of pDNA [32], however, mRNA does not need to be internalized into the nuclei of these cells, allowing efficient protein expression in the cells. Indeed, in our preliminary study, pDNA exhibited much less transgene expression after intranasal administration, even when using the same polyplex nanomicelle (unpublished data). In contrast, intranasal mRNA administration provided diffuse GFP expression in the lamina propria beneath the basement membrane of epithelial cells (Fig. 2). The lamina propria primarily consists of non-dividing cells, such as nerve and inflammatory cells, interspersed among connective tissue and blood vessels. Although we did not identify individual GFP-positive cells in our histological sections, the diffuse expression of GFP in the lamina propria strongly suggested that mRNA had been successfully introduced into non-dividing cells.

Another advantage of using mRNA is the early onset of protein expression. It has been reported that the protein expression was detectable even 15 min after mRNA transfection, much faster than that after pDNA transfection [33]. In this study, protein expression in the nasal cavity was obvious a few hours after intranasal mRNA administration (Fig. 1A, B), clearly suggesting the rapid onset of protein expression in nasal tissues.

It is notable that the duration of protein expression would tend to be shorter with mRNA considering its rapid degradation [6,34]. Although little is known about the mechanisms underlying translation control in individual cells, a few studies have reported that the half-lives of mRNA in the cytoplasm were generally in the range of hours [35–37], indicating the very transient manner of protein expression from a single mRNA molecule.

Considering these features of mRNA, the roles of polyplex nanomicelles are not limited to transporting mRNA to target cells by overcoming the barriers in the nasal cavity, including the mucous layer, epithelial membrane and associated junctional barriers. These nanomicelles are also likely to stably retain mRNA in their core, even after they are internalized into target cells, thereby continuously

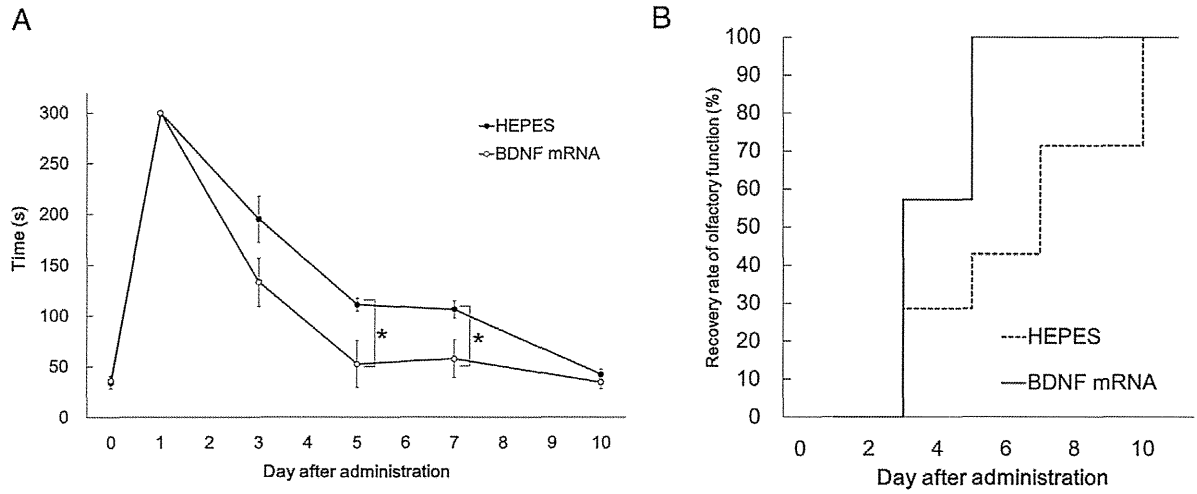

Fig. 4. Behavioral assessments of olfactory function. Olfactory sensations were evaluated with a buried food test to determine the amount of time required for mice to uncover food. (A) Average time required to uncover food of mice that received BDNF-expressing mRNA (open circle) and control mice that received HEPES buffer (closed circle). (B) Percentages of mice that showed curative recovery (could uncover food within 120 s). Statistical analyses were performed by two-tailed Mann–Whitney U test, *, $p < 0.05$. Results are means ± SEMs ($n = 7$).

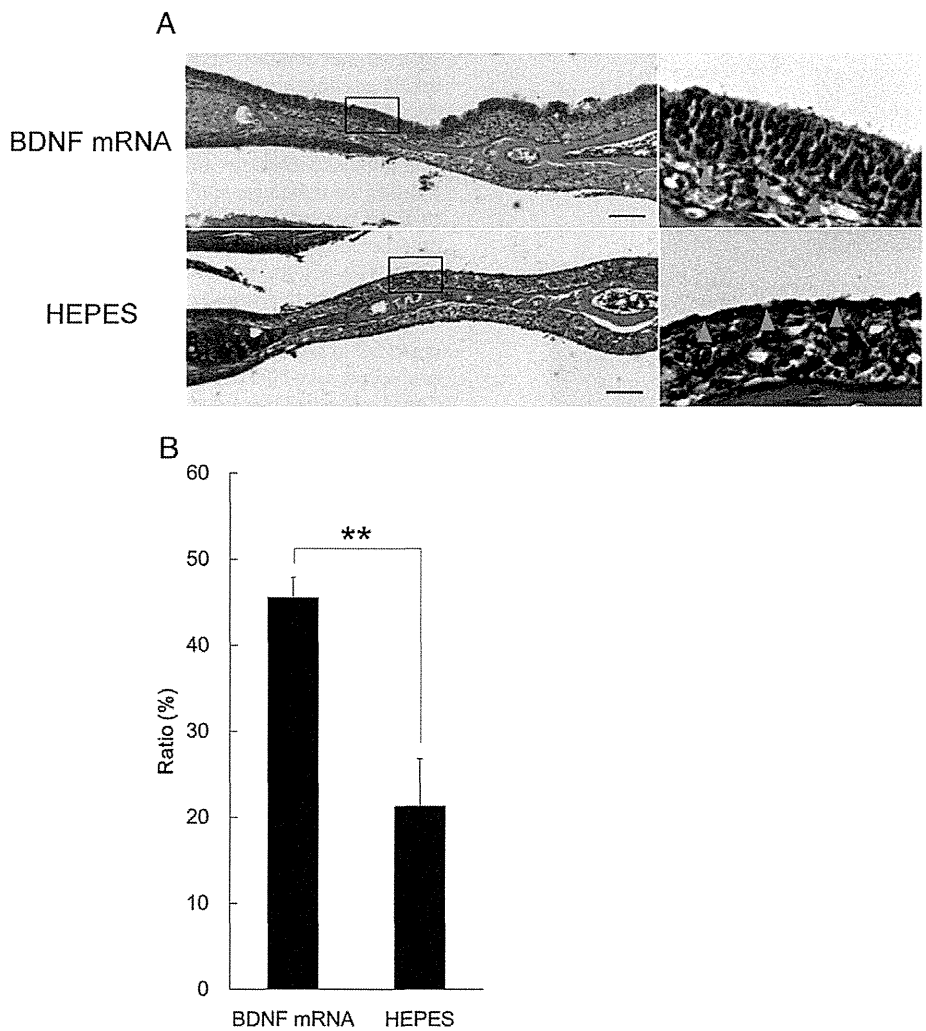

Fig. 5. Histopathological examination of the damaged olfactory epithelium. Mice were sacrificed and decapitated 24 h after administering GFP-expressing mRNA. The mandibles were discarded, and the trimmed heads were skinned. Serial sections (thickness, 5 μm) at the level of the anterior end of the olfactory bulb were prepared. These sections were stained with hematoxylin and eosin (H&E). (A) A representative image of a mouse that received BDNF-expressing mRNA or HEPES buffer. Green arrows indicate the basilar membranes. Scale bar: 100 μm. (B) Area ratios that were covered by the intact olfactory epithelium. Statistical analyses were performed by two-tailed Student's t-test, **, $p < 0.01$. Results are means ± SEMs ($n = 4$).

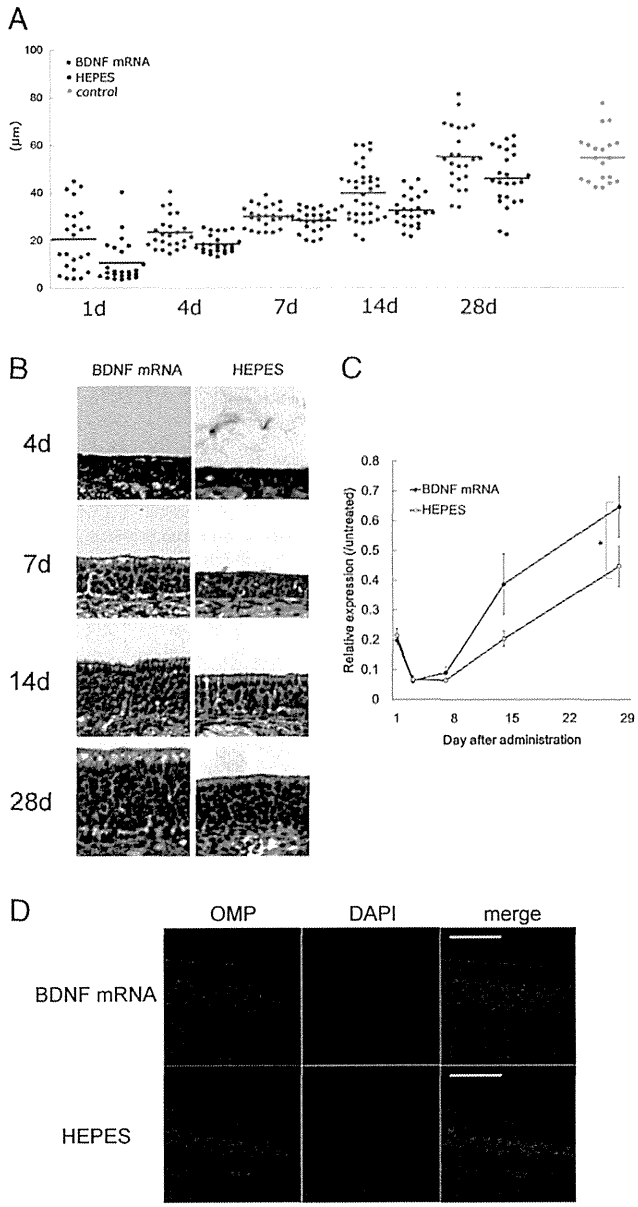

Fig. 6. Long-term effects of BDNF-expressing mRNA on the olfactory epithelium. (A) Thickness of the olfactory epithelium. The thickness of the epithelium was measured via the histological sections by determining the distance between the basilar membrane and the top of the cell layer of the nasal septum. Blue: Mice that received BDNF-expressing mRNA-loaded polyplex nanomicelles, red: Those received HEPES buffer, green: Normal mice that were not injected with methimazole.(B) Representative images of the olfactory epithelium from mice that received BDNF-expressing mRNA-loaded polyplex nanomicelles or HEPES buffer.(C) OMP mRNA expression levels in nasal tissues expression in the nasal tissue evaluated using real-time quantitative PCR (qPCR). Statistical analyses were performed by two-tailed Student's t-test, *, $p < 0.05$. Results are means ± SEMs ($n = 7$).(D) Representative images of immunostained sections of olfactory epithelium using an anti-OMP antibody 28 days after administering of BDNF-expressing mRNA-loaded polyplex nanomicelles or HEPES buffer. Scale bar: 50 μm.

releasing intact mRNA in the cytoplasm. This property enables sustained protein expression in the cells for nearly two days. Thus, it would be expected that therapeutic proteins would be continuously provided for the nasal tissues by once-daily administration of mRNA-loaded nanomicelles.

These aspects of rapidly-emerging and sustained activity considerably augment the usefulness of mRNA for treating neurological disorders. Indeed, BDNF protein has a half-life of only a few minutes in rat plasma [38], and showed no therapeutic effect on olfactory dysfunction by intranasal administration [39]. Direct administration of BDNF may not attain significant therapeutic outcome for treating neurological disorders because prolonged action in a sustained manner is needed to acquire the neurological recovery. Thus, modification of protein to elongate the half-life, or the use of adjunctive means, such as continuous infusion devices or incorporation into an artificial matrix for controlled drug release, is required because the proteins generally have poor stability under physiological conditions [40,41]. However, since these devices involve invasive procedures, therapeutic outcomes are not easy to achieve, particularly for neural tissues that require highly delicate manipulations.

From the toxicological standpoints, it is important that intranasal mRNA administration using the nanomicelles induced minimal immune responses, returning to the normal state 24 h after administration. We previously reported that the nanomicelles effectively suppressed mRNA immunogenicity, even when using wild-type mRNA, after administration into the subarachnoid space [14]. Because the nasal cavity is a much more sensitive site for foreign materials, in this study, we used a modified mRNA that exhibited reduced immunogenicity by interfering with the interaction of mRNA with Toll-like receptors [11]. Indeed, even this modified form of naked mRNA triggered strong immune responses after administration into nasal tissues. However, the identical mRNA administered with the nanomicelles induced significantly reduced immune responses (Fig. 3), without any apparent damage to nasal tissues (Fig. 2). Thus, it is reasonable to assume that the nanomicelles are effective to regulate mRNA immunogenicity, further increasing the usefulness of mRNA for therapeutic purposes.

BDNF is a member of the neurotrophin family and its effects include pro-survival activities for neurons under various pathological conditions [42–45], and synaptic repair capacity to enhance synaptic transmission, facilitate synaptic plasticity and promote synaptic growth [46, 47]. In agreement with its expected functions, the effects of BDNF demonstrated in this study appeared to include two phases. The first was a neuroprotective effect against methimazole-induced damage, as indicated by the well preserved olfactory epithelial structure and early recovery of olfactory sensations within a few days after introducing BDNF-expressing mRNA. Although it was difficult to directly determine the amount of BDNF in the nasal tissue of small animals like mice by ELISA, a therapeutic quantity of BDNF protein may be provided in a sustained manner in the nasal cavity through the expression of BDNF-coded mRNA for 5 consecutive days. The latter phase of BDNF effects involved enhancing the regeneration of mature olfactory neurons with significant differences from the untreated controls, as reflected by the increased thickness of the olfactory epithelium and enhanced OMP signals (Fig. 6). After neurological damage, OMP signals gradually decrease for a week during cell dropout from the epithelium, then shows a slow recovery in parallel with the mitoses of basal cells [48]. In this study, it is interesting that these effects were observed for a few weeks after mRNA administration, although the period of administration was limited to 5 days. Thus, the supply of exogenous BDNF protein to nasal tissues was likely to be terminated approximately a week after inducing an olfactory dysfunction. A reasonable speculation is that BDNF expressed by mRNA not only stimulated the olfactory neurons for enhanced regeneration, but also effectively ameliorated the pathological conditions in nasal tissues to be suitable for nerve regeneration.

In conclusion, we used mRNA to treat olfactory dysfunction by in vivo intranasal administration using polyplex nanomicelles. mRNA provided efficient, sustained protein expression for nasal tissues, particularly in the lamina propria. BDNF-expressing mRNA remarkably enhanced the neurological recovery of olfactory function along with repairing the olfactory epithelium to a nearly normal architecture. These results indicate the feasibility and safety of using mRNA and provide a novel strategy of mRNA-based therapy for neurogenic disorders.

Acknowledgments

This work was financially supported in part by JSPS KAKENHI Grant-in-Aid for Scientific Research (B) (Grant Number 24300170 (K.I.)), the Center of Innovation (COI) Program, the S-innovation Program from Japan Science and Technology Agency (JST), and the JSPS Core-to-Core Program, A. Advanced Research Networks. We thank Katsue Morii, Satomi Ogura, Asuka Miyoshi and Sae Suzuki (The University of Tokyo) for technical assistance.

References

[1] A. Kishino, Y. Ishige, T. Tatsuno, C. Nakayama, H. Noguchi, BDNF prevents and reverses adult rat motor neuron degeneration and induces axonal outgrowth, Exp. Neurol. 144 (1997) 273–286.
[2] B. Connor, M. Dragunow, The role of neuronal growth factors in neurodegenerative disorders of the human brain, Brain Res. Brain Res. Rev. 27 (1998) 1–39.
[3] E.N. Hammond, W. Tetzlaff, P. Mestres, K.M. Giehl, BDNF, but not NT-3, promotes long-term survival of axotomized adult rat corticospinal neurons in vivo, Neuroreport 10 (1999) 2671–2675.
[4] K.M. Giehl, S. Rohrig, H. Bonatz, M. Gutjahr, B. Leiner, I. Bartke, Q. Yan, L.F. Reichardt, C. Backus, A.A. Welcher, K. Dethleffsen, P. Mestres, M. Meyer, Endogenous brain-derived neurotrophic factor and neurotrophin-3 antagonistically regulate survival of axotomized corticospinal neurons in vivo, J. Neurosci. 21 (2001) 3492–3502.
[5] A. Yamamoto, M. Kormann, J. Rosenecker, C. Rudolph, Current prospects for mRNA gene delivery, Eur. J. Pharm. Biopharm. 71 (2009) 484–489.
[6] G. Tavernier, O. Andries, J. Demeester, N.N. Sanders, S.C. De Smedt, J. Rejman, mRNA as gene therapeutic: how to control protein expression, J. Control. Release 150 (2011) 238–247.
[7] T.H. Howell, J. Fiorellini, A. Jones, M. Alder, P. Nummikoski, M. Lazaro, L. Lilly, D. Cochran, A feasibility study evaluating rhBMP-2/absorbable collagen sponge device for local alveolar ridge preservation or augmentation, Int. J. Periodontics Restor. Dent. 17 (1997) 124–139.
[8] M. Zhao, Z. Zhao, J.T. Koh, T. Jin, R.T. Franceschi, Combinatorial gene therapy for bone regeneration: cooperative interactions between adenovirus vectors expressing bone morphogenetic proteins 2, 4, and 7, J. Cell. Biochem. 95 (2005) 1–16.
[9] F. Heil, H. Hemmi, H. Hochrein, F. Ampenberger, C. Kirschning, S. Akira, G. Lipford, H. Wagner, S. Bauer, Species-specific recognition of single-stranded RNA via toll-like receptor 7 and 8, Science 303 (2004) 1526–1529.
[10] K. Kariko, H. Ni, J. Capodici, M. Lamphier, D. Weissman, mRNA is an endogenous ligand for Toll-like receptor 3, J. Biol. Chem. 279 (2004) 12542–12550.
[11] M.S. Kormann, G. Hasenpusch, M.K. Aneja, G. Nica, A.W. Flemmer, S. Herber-Jonat, M. Huppmann, L.E. Mays, M. Illenyi, A. Schams, M. Griese, I. Bittmann, R. Handgretinger, D. Hartl, J. Rosenecker, C. Rudolph, Expression of therapeutic proteins after delivery of chemically modified mRNA in mice, Nat. Biotechnol. 29 (2011) 154–157.
[12] K. Kariko, H. Muramatsu, J.M. Keller, D. Weissman, Increased erythropoiesis in mice injected with submicrogram quantities of pseudouridine-containing mRNA encoding erythropoietin, Mol. Ther. 20 (2012) 948–953.
[13] L. Zangi, K.O. Lui, A. von Gise, Q. Ma, W. Ebina, L.M. Ptaszek, D. Spater, H. Xu, M. Tabebordbar, R. Gorbatov, B. Sena, M. Nahrendorf, D.M. Briscoe, R.A. Li, A.J. Wagers, D.J. Rossi, W.T. Pu, K.R. Chien, Modified mRNA directs the fate of heart progenitor cells and induces vascular regeneration after myocardial infarction, Nat. Biotechnol. 31 (2013) 898–907.
[14] S. Uchida, K. Itaka, H. Uchida, K. Hayakawa, T. Ogata, T. Ishii, S. Fukushima, K. Osada, K. Kataoka, In vivo messenger RNA introduction into the central nervous system using polyplex nanomicelle, PLoS One 8 (2013) e56220.
[15] N. Kanayama, S. Fukushima, N. Nishiyama, K. Itaka, W.D. Jang, K. Miyata, Y. Yamasaki, U.I. Chung, K. Kataoka, A PEG-based biocompatible block catiomer with high buffering capacity for the construction of polyplex micelles showing efficient gene transfer toward primary cells, ChemMedChem 1 (2006) 439–444.
[16] K. Itaka, T. Ishii, Y. Hasegawa, K. Kataoka, Biodegradable polyamino acid-based polycations as safe and effective gene carrier minimizing cumulative toxicity, Biomaterials 31 (2010) 3707–3714.
[17] K. Itaka, K. Kataoka, Progress and prospects of polyplex nanomicelles for plasmid DNA delivery, Curr. Gene Ther. 11 (2011) 457–465.
[18] K. Miyata, N. Nishiyama, K. Kataoka, Rational design of smart supramolecular assemblies for gene delivery: chemical challenges in the creation of artificial viruses, Chem. Soc. Rev. 41 (2012) 2562–2574.
[19] M.B. Genter, N.J. Deamer, B.L. Blake, D.S. Wesley, P.E. Levi, Olfactory toxicity of methimazole: dose–response and structure–activity studies and characterization of flavin-containing monooxygenase activity in the Long-Evans rat olfactory mucosa, Toxicol. Pathol. 23 (1995) 477–486.
[20] A. Mackay-Sim, P. Kittel, Cell dynamics in the adult mouse olfactory epithelium: a quantitative autoradiographic study, J. Neurosci. 11 (1991) 979–984.
[21] M.E. Buckland, A.M. Cunningham, Alterations in expression of the neurotrophic factors glial cell line-derived neurotrophic factor, ciliary neurotrophic factor and brain-derived neurotrophic factor, in the target-deprived olfactory neuroepithelium, Neuroscience 90 (1999) 333–347.
[22] F. Feron, J. Bianco, I. Ferguson, A. Mackay-Sim, Neurotrophin expression in the adult olfactory epithelium, Brain Res. 1196 (2008) 13–21.
[23] H.R. Costantino, L. Illum, G. Brandt, P.H. Johnson, S.C. Quay, Intranasal delivery: physicochemical and therapeutic aspects, Int. J. Pharm. 337 (2007) 1–24.
[24] G. Wang, J. Zabner, C. Deering, J. Launspach, J. Shao, M. Bodner, D.J. Jolly, B.L. Davidson, P.B. McCray Jr., Increasing epithelial junction permeability enhances gene transfer to airway epithelia In vivo, Am. J. Respir. Cell Mol. Biol. 22 (2000) 129–138.
[25] Y. Nishibe, A. Nagano, Y. Uejima, Nasal suspensions with low osmolality and drug permeability, Jibi Inkoka Tembo 45 (Suppl. 1) (2002) 46–49.
[26] C. Dufes, J.C. Olivier, F. Gaillard, A. Gaillard, W. Couet, J.M. Muller, Brain delivery of vasoactive intestinal peptide (VIP) following nasal administration to rats, Int. J. Pharm. 255 (2003) 87–97.
[27] S. Yu, Y. Zhao, F. Wu, X. Zhang, W. Lu, H. Zhang, Q. Zhang, Nasal insulin delivery in the chitosan solution: in vitro and in vivo studies, Int. J. Pharm. 281 (2004) 11–23.
[28] T. Kawamoto, Use of a new adhesive film for the preparation of multi-purpose fresh-frozen sections from hard tissues, whole-animals, insects and plants, Arch. Histol. Cytol. 66 (2003) 123–143.
[29] M. Yang, J.N. Crawley, Simple behavioral assessment of mouse olfaction, in: Jacqueline N. Crawley, et al., (Eds.)Current Protocols in Neuroscience/Editorial Board, 2009 (Chapter 8, Unit 8 24).
[30] K. Suzukawa, K. Kondo, K. Kanaya, T. Sakamoto, K. Watanabe, M. Ushio, K. Kaga, T. Yamasoba, Age-related changes of the regeneration mode in the mouse peripheral olfactory system following olfactotoxic drug methimazole-induced damage, J. Comp. Neurol. 519 (2011) 2154–2174.
[31] G.A. Graziadei, R.S. Stanley, P.P. Graziadei, The olfactory marker protein in the olfactory system of the mouse during development, Neuroscience 5 (1980) 1239–1252.
[32] A. Subramanian, P. Ranganathan, S.L. Diamond, Nuclear targeting peptide scaffolds for lipofection of nondividing mammalian cells, Nat. Biotechnol. 17 (1999) 873–877.
[33] J. Rejman, G. Tavernier, N. Bavarsad, J. Demeester, S.C. De Smedt, mRNA transfection of cervical carcinoma and mesenchymal stem cells mediated by cationic carriers, J. Control. Release 147 (2010) 385–391.
[34] R. Parker, U. Sheth, P bodies and the control of mRNA translation and degradation, Mol. Cell 25 (2007) 635–646.
[35] L.V. Sharova, A.A. Sharov, T. Nedorezov, Y. Piao, N. Shaik, M.S. Ko, Database for mRNA half-life of 19 977 genes obtained by DNA microarray analysis of pluripotent and differentiating mouse embryonic stem cells, DNA Res. 16 (2009) 45–58.
[36] B. Schwanhausser, D. Busse, N. Li, G. Dittmar, J. Schuchhardt, J. Wolf, W. Chen, M. Selbach, Global quantification of mammalian gene expression control, Nature 473 (2011) 337–342.
[37] H. Tani, N. Akimitsu, Genome-wide technology for determining RNA stability in mammalian cells: historical perspective and recent advantages based on modified nucleotide labeling, RNA Biol. 9 (2012) 1233–1238.
[38] J.F. Poduslo, G.L. Curran, Permeability at the blood–brain and blood–nerve barriers of the neurotrophic factors: NGF, CNTF, NT-3, BDNF, Brain Res. Mol. Brain Res. 36 (1996) 280–286.
[39] H. Yasuno, K. Fukazawa, T. Fukuoka, E. Kondo, M. Sakagami, K. Noguchi, Nerve growth factor applied onto the olfactory epithelium alleviates degenerative changes of the olfactory receptor neurons following axotomy, Brain Res. 887 (2000) 53–62.
[40] R.G. Soderquist, E.D. Milligan, E.M. Sloane, J.A. Harrison, K.K. Douvas, J.M. Potter, T.S. Hughes, R.A. Chavez, K. Johnson, L.R. Watkins, M.J. Mahoney, PEGylation of brain-derived neurotrophic factor for preserved biological activity and enhanced spinal cord distribution, J. Biomed. Mater. Res. A 91 (2009) 719–729.
[41] F. Huang, Z. Yin, D. Wu, J. Hao, Effects of controlled release of brain-derived neurotrophic factor from collagen gel on rat neural stem cells, Neuroreport 24 (2013) 101–107.
[42] D. Lindholm, G. Dechant, C.P. Heisenberg, H. Thoenen, Brain-derived neurotrophic factor is a survival factor for cultured rat cerebellar granule neurons and protects them against glutamate-induced neurotoxicity, Eur. J. NeuroSci. 5 (1993) 1455–1464.
[43] L. Tong, R. Perez-Polo, Brain-derived neurotrophic factor (BDNF) protects cultured rat cerebellar granule neurons against glucose deprivation-induced apoptosis, J. Neural Transm. 105 (1998) 905–914.
[44] P. Tandon, Y. Yang, K. Das, G.L. Holmes, C.E. Stafstrom, Neuroprotective effects of brain-derived neurotrophic factor in seizures during development, Neuroscience 91 (1999) 293–303.
[45] S. Arancibia, M. Silhol, F. Mouliere, J. Meffre, I. Hollinger, T. Maurice, L. Tapia-Arancibia, Protective effect of BDNF against beta-amyloid induced neurotoxicity in vitro and in vivo in rats, Neurobiol. Dis. 31 (2008) 316–326.
[46] J.A. Kleim, S. Chan, E. Pringle, K. Schallert, V. Procaccio, R. Jimenez, S.C. Cramer, BDNF val66met polymorphism is associated with modified experience-dependent plasticity in human motor cortex, Nat. Neurosci. 9 (2006) 735–737.
[47] B. Fritsch, J. Reis, K. Martinowich, H.M. Schambra, Y. Ji, L.G. Cohen, B. Lu, Direct current stimulation promotes BDNF-dependent synaptic plasticity: potential implications for motor learning, Neuron 66 (2010) 198–204.
[48] J. Harding, P.P. Graziadei, G.A. Monti Graziadei, F.L. Margolis, Denervation in the primary olfactory pathway of mice. IV. Biochemical and morphological evidence for neuronal replacement following nerve section, Brain Res. 132 (1977) 11–28.

Journal of Controlled Release 197 (2015) 1–9

Contents lists available at ScienceDirect

Journal of Controlled Release

journal homepage: www.elsevier.com/locate/jconrel

Intrathecal injection of a therapeutic gene-containing polyplex to treat spinal cord injury

Kentaro Hayakawa [a,b], Satoshi Uchida [c], Toru Ogata [a], Sakae Tanaka [b], Kazunori Kataoka [c,d,*], Keiji Itaka [b,c,**]

[a] Department of Rehabilitation for the Movement Functions, Research Institute, National Rehabilitation Center for the Persons with Disabilities, Saitama, Japan
[b] Sensory and Motor System Medicine, Faculty of Medicine, The University of Tokyo, Tokyo, Japan
[c] Laboratory of Clinical Biotechnology, Center for Disease Biology and Integrative Medicine, Graduate School of Medicine, The University of Tokyo, Tokyo, Japan
[d] Department of Materials Engineering, Graduate School of Engineering, The University of Tokyo, Tokyo, Japan

ARTICLE INFO

Article history:
Received 11 June 2014
Accepted 27 October 2014
Available online 4 November 2014

Keywords:
Spinal cord injury
Brain-derived neurotrophic factor (BDNF)
Gene delivery
Polyplex
Intrathecal injection

ABSTRACT

Spinal cord injury (SCI) is a serious clinical problem that suddenly deprives patients of neurologic function and drastically diminishes their quality of life. Gene introduction has the potential to be effective for various pathological states of SCI because various proteins can be produced just by modifying nucleic acid sequences. In addition, the sustainable protein expression allows to maintain its concentration at an effective level at the target site in the spinal cord. Here we propose an approach using a polyplex system composed of plasmid DNA (pDNA) and a cationic polymer, poly{*N*′-[*N*-(2-aminoethyl)-2-aminoethyl]aspartamide} [PAsp(DET)], that has high capacity to promote endosome escape and the long-term safety by self-catalytically degrading within a few days. We applied brain-derived neurotrophic factor (BDNF)-expressing pDNA for SCI treatment by intrathecal injection of PAsp(DET)/pDNA polyplex. A single administration of polyplex for experimental SCI provided sufficient therapeutic effects including prevention of neural cell death and enhancement of motor function recovery. This lasted for a few weeks after SCI, demonstrating the capability of this system to express BDNF in a safe and responsible manner for treatment of various pathological states in SCI.

1. Introduction

Spinal cord injury (SCI) is a serious clinical problem that suddenly deprives patients of neurologic function and drastically diminishes their quality of life [1,2]. Initial mechanical trauma to the spinal cord is followed by secondary injury, which is the progression of tissue damage for several days due to delayed neural cell death around the original site of injury [3–5]. Because initial injury has already occurred before hospital arrival, the therapeutic target has been focused on attenuation of secondary injury. However, there are few pharmacological strategies showing solid evidence of therapeutic effectiveness in clinical settings. One reason for this is the complex pathophysiology of secondary injury such as inflammatory responses, a variety of molecules inhibiting regeneration, and a lack of trophic support [6–10]. In addition, the pathophysiology is constant or increased for several days. Thus, therapeutic molecules need to be effective and sustainable for various pathological states in secondary injury. However, it is not only difficult to choose adequate therapeutic molecules, but it is also difficult to maintain the concentration of the molecules at an effective level at the target site in the spinal cord [11].

Gene introduction has the potential to be effective for the treatment of SCI because various proteins can be produced just by modifying nucleic acid sequences. In addition, sustainable protein expression resulting from an introduced gene is apparently beneficial for regulating the complex pathophysiology of SCI. For this purpose, viral vectors such as herpes simplex virus vectors had been evaluated [12]. However, viral vectors still have problems surrounding their genotoxicity and immunogenicity, hampering their administration for acute and serious states of SCI [13–15].

A non-viral system that can introduce genes to express therapeutic molecules has high potential for the treatment of SCI. Since neural tissue is mostly composed of highly differentiated, non-dividing cells, the system needs to have a high level of safety so as not to impede long-term neural function after gene introduction.

In this context, we propose an approach using a polyplex system composed of plasmid DNA (pDNA) and cationic polymers [16,17]. The polyplex system can protect pDNA from nuclease attack and increase cellular uptake through electrostatic interactions between a cationic

* Correspondence to: K. Kataoka, Department of Materials Engineering, Graduate School of Engineering, The University of Tokyo, 7-3-1 Hongo, Bunkyo-ku, Tokyo 113-0033, Japan. Tel.: +81 3 5841 7138; fax: +81 3 5841 7139.
** Correspondence to: K. Itaka, Laboratory of Clinical Biotechnology, Center for Disease Biology and Integrative Medicine, Graduate School of Medicine, The University of Tokyo, 7-3-1 Hongo, Bunkyo-ku, Tokyo 113-0033, Japan. Tel.: +81 3 5841 1418; fax: +81 3 5841 1419.
E-mail addresses: kataoka@bmw.t.u-tokyo.ac.jp (K. Kataoka), itaka-ort@umin.net (K. Itaka).

http://dx.doi.org/10.1016/j.jconrel.2014.10.027
0168-3659/

polyplex and the anionic cell membrane. One of the critical barriers in achieving good gene expression is the inefficient translocation from endosomes to the cytoplasm. The capacity of polymers to buffer acidic environments in the endosomes, typically represented by polyethylenimine (PEI) [18], has been intensely investigated to increase the efficiency of translocation, although the toxicity of the polymers has hampered their application for therapeutic purposes [19]. Our original cationic polymer, poly{*N*′-[*N*-(2-aminoethyl)-2-aminoethyl] aspartamide} [PAsp(DET)] [20,21], effectively solves the safety issues by self-catalytically degrading within a few days, minimizing the cumulative toxicity caused by the polymers remaining in the cells [22]. Besides its high capacity to promote endosome escape, it was revealed by a pharmacogenomic analysis that PAsp(DET) did not alter the expression profiles of endogenous genes after introduction into cells, confirming the long-term safety of PAsp(DET) in not affecting innate cell function [23,24].

The purpose of this study is to investigate the availability of the polyplex system for the treatment of SCI. As a proof-of-concept study, we used Brain-derived neurotrophic factor (BDNF) as a therapeutic agent. BDNF is a member of neurotrophins, which have gained much attention for exerting diverse effects as a trophic support in treating SCI [25,26]. In animal studies, recombinant BDNF protein showed therapeutic effects by enhancing neural cell survival and axonal regeneration in SCI by intrathecal infusion [27,28]. However, multiple or continuous administrations using a catheter are usually required to maintain effective concentrations of BDNF protein at the injured site, and this would cause complications such as scar formation at the catheter tip, which can lead to infusion failure and damage to the spinal cord caused by the catheter itself [29,30].

In this study, we applied BDNF-expressing pDNA for SCI treatment by intrathecal injection of PAsp(DET)/pDNA polyplex. As shown later, a single administration of polyplex provided sufficient therapeutic effects including prevention of neural cell death and enhancement of motor function recovery. This lasted for a few weeks after SCI, demonstrating the capability of this system to express BDNF in a safe and responsible manner for treatment of various pathological states in SCI.

2. Materials and methods

2.1. Materials

Plasmid DNA (pDNA) encoding luciferase (pGL4.13: Promega, Madison, WI, USA) and brain-derived neurotrophic factor (BDNF) (pUNO1-hBDNFa: InvivoGen, San Diego, CA, USA) were amplified in competent DH5α *Escherichia coli* and purified using NucleoBond Xtra EF (Nippon Genetics, Tokyo, Japan). The pDNA concentration was determined by reading the absorbance at 260 nm. Linear polyethyleneimine (LPEI) (Exgen 500, *in vivo*; MW = 22,000) was obtained from MBI Fermentas (Burlington, ON, Canada). Lipofectamine 2000 transfection reagent was from Thermo Fisher Scientific (Waitham, MA, USA). PAsp(DET) polymer was synthesized as described previously [20]. By ^{1}H-NMR analysis, the polymerization degree of PAsp(DET) was determined to be 52.

2.2. Animals

C57BL6/J mice (female, eight-weeks-old) were purchased from Charles River Laboratories (Yokohama, Japan). The mice were allowed to feed and drink *ad libitum* on a 12-h light/dark cycle prior to experimentation. All animal protocols were conducted with the approval of the Animal Care and Use Committee of the University of Tokyo.

2.3. Preparation of polyplex or lipoplex containing pDNA

To form PAsp(DET)/pDNA polyplex, PAsp(DET) polymer and pDNA were separately dissolved in 10 mM HEPES buffer at pH 7.4. The polyplex was obtained by simply mixing both solutions at N/P ([total amines in polymer]/[DNA phosphates]) ratio of 8. LPEI-based pDNA carrier was prepared by mixing LPEI and pDNA solution at N/P ratio of 6, which is recommended as an optimal transfection condition by the manufacturer. Lipoplex was formed following the manufacturer's protocol by mixing Lipofectamine 2000 and pDNA. The final pDNA concentration was adjusted to 200 μg/ml for all samples.

2.4. Intrathecal injection of pDNA solution

Mice were anesthetized with isoflurane (Escain: Mylan, Canonsburg, PA, USA). The skin was incised so that the superficial fat could be pried apart to dissect the muscle tissue and expose the lumbar laminae. An injection needle was inserted into the dural space from the interlaminar space between L4 and L5, and 10 μl of solution containing 2 μg pDNA was injected in 60 s with Hamilton syringe (Sigma-Aldrich, St. Louis, MO, USA). The tip of the needle was kept at the injection site for 5 min to prevent leakage of cerebrospinal fluid (CSF).

2.5. Experimental spinal cord injury

Twenty-four hours after the injection of carrier solutions, mice were anesthetized with sodium pentobarbital (50 mg/kg) (Somno-pentyl: Kyoritsu Seiyaku, Tokyo, Japan). The thoracic laminae were exposed, and laminectomy was performed at the level of the 9th thoracic vertebra. A contusion SCI was induced using Infinite Horizons Impactor (Precision Systems and Instrumentation LLC, Fairfax, VA, USA) with an impact force of 60 kilodynes. Mice underwent daily check for general health, mobility within the cage, wounds, infections, and autophagy of the toes throughout the experiment. Bladders were manually pressed twice daily for the first week after operation and once daily until no longer needed.

2.6. Evaluation of luciferase expression

In vivo luciferase expression was evaluated using the IVIS™ Imaging System (Xenogen, Alameda, CA, USA) after intraperitoneal injection of D-luciferin (150 mg/kg, Sumisho Pharmaceuticals International, Tokyo, Japan), following the manufacturer's protocol.

2.7. Measurement of proinflammatory cytokines

Total RNA was isolated from extracted neural tissues using the RNeasy Mini Preparation Kit (Qiagen, Hilden, Germany). The gene expression of proinflammatory cytokines was analyzed by real-time quantitative PCR using an ABI Prism 7500 Sequence Detector (Applied Biosystems, Foster City, CA, USA), and TaqMan Gene Expression Assays (Mm00443258_m1 for tumor necrosis factor (TNF)-α, Mm00446

Table 1
CatWalk parameters.

CatWalk parameters	Explanation
Print area	Total surface area contacted by the hindpaw during the complete stance duration
Mean intensity	Mean intensity of the pixels forming the maximum area
Stride length	Distance between the placement of a hindpaw and the subsequent placement of the same paw
Base of support (BOS)	Distance between two hindpaws, as measured perpendicular to the walking direction
Print positions	Distance between the placement of a hindpaw and the ipsilateral frontpaw placed just before

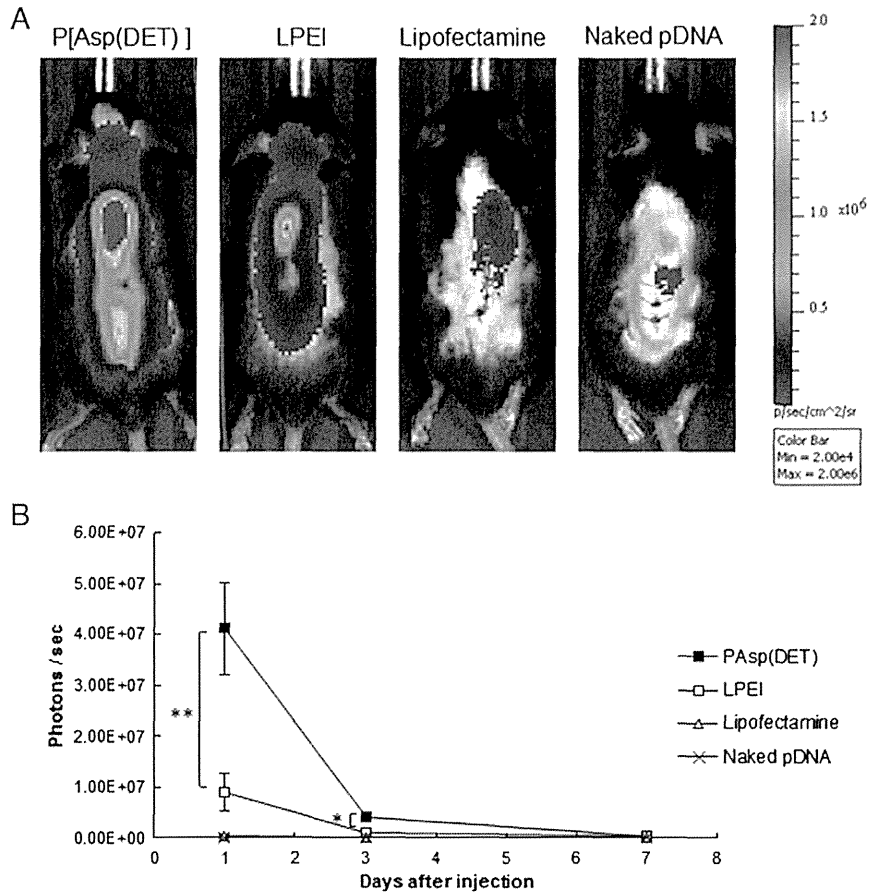

Fig. 1. Luciferase expression at spinal cord of normal mice after intrathecal injection of luciferase-expressing pDNA using PAsp(DET), LPEI, Lipofectamine, or in the form of naked pDNA. (A) Representative IVIS images of mice 1 day after injection. (B) Time course of luciferase expression quantified from the IVIS images. Data are expressed as means ± SEMs ($n = 5$), $^{**}p < 0.01$, $^{*}p < 0.05$ vs. LPEI.

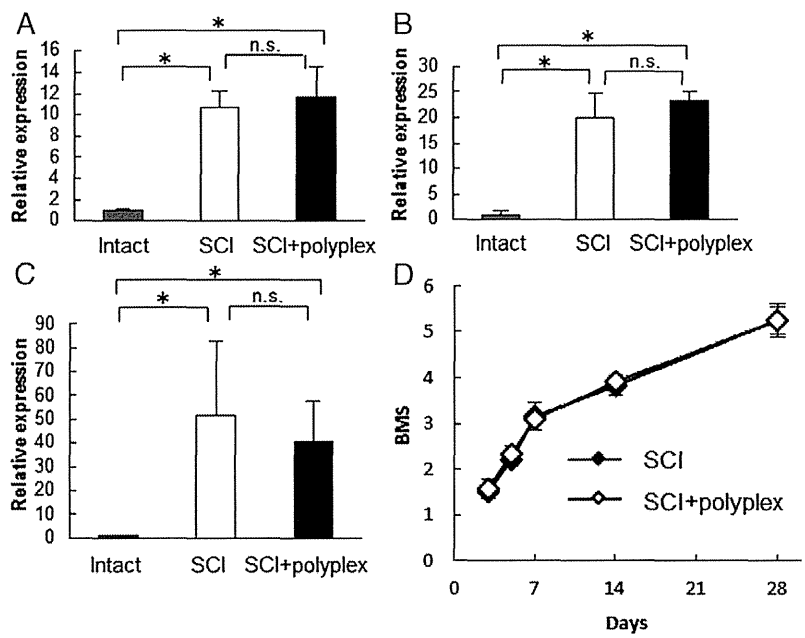

Fig. 2. Proinflammatory cytokines gene expression 24 h after intrathecal injection of PAsp(DET)/pDNA (luciferase) polyplexes. The messenger RNA (mRNA) expression of TNF-α (A), IL-6 (B), and IL-1β (C) in the lower thoracic spinal cord region was evaluated by real-time quantitative PCR. Data are expressed as a relative value to that from intact spinal cord region. Data are expressed as means ± SEMs (intact control: $n = 3$, the others: $n = 5$), $^{*}p < 0.05$. (D) Spontaneous recovery of walking motion that was evaluated by BMS scoring after inducing experimental SCI ($n = 6$). Intrathecal injection did not affect the recovery.

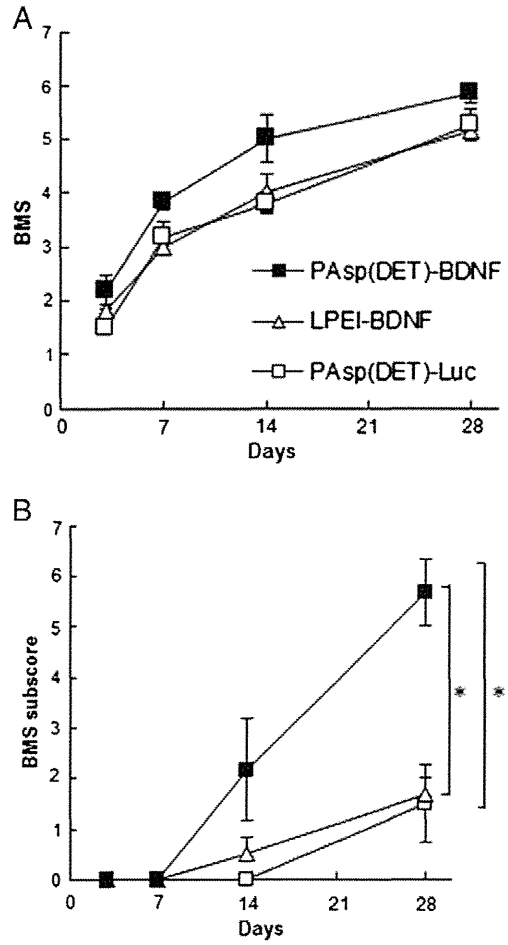

Fig. 3. Analysis of walking motion by BMS scoring after intrathecal injection of BDNF-expressing pDNA using PAsp(DET) (close square), LPEI (triangle), or luciferase-expressing pDNA using PAsp(DET) (open square), concomitantly with the induction of experimental SCI. (A) BMS, (B) BMS subscore. Data are expressed as means ± SEMs ($n = 6$), $^*p < 0.05$.

190_m1 for interleukin (IL)-6, Mm00434228_m1 for IL-1β, and Mm00607939 for β-actin).

2.8. Behavioral assessments

Hind-limb motor function was evaluated using two separate procedures, the Basso Mouse Scale (BMS) open field locomotor test and a computerized gait analysis using CatWalk gait analysis system (Noldus, Wageningen, Netherlands). In the former, two blinded persons assessed parameters of stepping frequency, coordination, paw position, trunk stability, and tail position, by scoring from 0 points (no ankle movement) to 9 points (complete functional recovery) [31]. In addition, since mice may not show formulaic recovery of motor function by correlation with the BMS scores, we also calculated BMS subscore by adding each score of the parameters described above. The scores of right and left hind limbs were averaged.

In the latter, we analyzed the walking pattern in a quantitative manner by assessing the parameters shown in Table 1, including those reflecting regularity and relative paw placement [32]. Each mouse was allowed to cross runway with a glass floor (L 50 cm × W 8 cm) in a darkened room. Footprints, illuminated with green LED light, were observed with a charge-coupled device (CCD) for following analyses with CatWalk XT 10.0 software (Noldus).

2.9. Evaluation of the cell apoptosis

We used the terminal deoxynucleotidyl transferase dUTP Nick-End Labeling (TUNEL) assay. Mice were perfused transcardially under deep ether anesthesia with buffered 4% paraformaldehyde. The spinal cords were removed and postfixed in 4% paraformaldehyde at 4 °C for 4 h, cryoprotected in buffered 20% sucrose at 4 °C for 24 h, 30% sucrose for 24 h, and were embedded in optimal cutting temperature compound (Sakura Finetek, Torrance, CA, USA). Frozen tissues were cut into 14 μm longitudinal sections with a cryostat and mounted on glass slides. The midline section was chosen and the apoptotic cells were labeled with TMR red using *In Situ* Cell Death Detection Kit (Roche Applied Science, Mannheim, Germany) following the manufacturer's protocol, then mounted with 4′,6-diamidino-2-phenylindole (Vector Laboratories, Burlingame, CA, USA). For counting of apoptotic cells, three areas were chosen in rostal, caudal, and ventral regions surrounding the spinal cord lesion (see Fig. 5A) for fluorescent microscopic observation using AxioVision (Carl Zeiss, Oberkochen, Germany) under ×200 magnification. The numbers of apoptotic cells and whole cells were counted using an image analyzer software (WinROOF: Mitani Co., Tokyo, Japan).

2.10. Evaluation of the tissue sparing

Frozen tissue sections were prepared as described in the previous section. Myelin and myelinated axons were stained with Luxol fast blue (LFB) solution [33]. Briefly, the sections were hydrated with 95% ethanol and de-fatted with 1:1 ethanol/chloroform, hydrated with 95% ethanol, and left in 0.1% LFB solution (Solvent blue: MP Biomedicals, Santa Ana, CA, USA) at 56 °C overnight. Then the sections were rinsed in 95% ethanol and distilled water, differentiated with the lithium carbonate solution and 95% ethanol, rinsed with distilled water, differentiated in 95% and 100% ethanol, cleared with xylene, and mounted. The section was viewed with an optical microscope (BX51: Olympus, Tokyo, Japan), and the images of the serial sections with an equal distance (200 μm) spanning ±400 μm from the epicenter were obtained with an image processing software (InStudio: Pixera Co., San Jose, CA, USA). For the quantification of tissue sparing in the images, the edges of the stained area were drawn with a pen tablet input device (Bamboo Pen: Wacom Co., Tokyo, Japan) and the surrounding area was automatically measured using WinROOF.

2.11. Statistical analysis

Statistical analyses were performed with an unpaired two-tailed Student's *t* test for single comparisons and one-way ANOVA for multiple comparisons. In all statistical analyses, values of $p < 0.05$ were considered statistically significant.

3. Results

3.1. Evaluation of transgene expression after intrathecal injection of pDNA/PAsp(DET) polyplex and other carriers

The gene introduction capacity and safety was evaluated by administering luciferase-expressing pDNA using cationic polymers (PAsp(DET) or LPEI), lipid (Lipofectamine), or naked pDNA. For each condition, an identical amount of pDNA was administered into normal mice by intrathecal injection from the interlaminar space between L4 and L5, followed by evaluation of luciferase expression by IVIS™ Imaging System.

One day after administration, the luciferase expression was well detected for polyplexes with PAsp(DET) and LPEI (Fig. 1A). PAsp(DET) showed significantly higher expression than LPEI (Fig. 1B), and the expression was observed along the spinal canal, suggesting that the polyplexes were distributed in the cerebral spinal fluid of subarachnoid space. Despite a marked decrease a few days after administration, the